Available online at www.sciencedirect.com
ScienceDirect
J. Vis. Commun. Image R. 18 (2007) 15–34
JOURNAL OF VISUAL Communication & IMAGE Representation
www.elsevier.com/locate/jvci

An efficient PCA-based color transfer method

Arash Abadpour [a], Shohreh Kasaei [b,*]

[a] Mathematics Science Department, Sharif University of Technology, Tehran, Iran
[b] Computer Engineering Department, Sharif University of Technology, Tehran, Iran

Received 2 August 2005; accepted 15 August 2006
Available online 2 October 2006

Abstract

Color information of natural images can be considered as a highly correlated vector space. Many different color spaces have been proposed in the literature with different motivations toward modeling and analysis of this stochastic field. Recently, color transfer among different images has been under investigation. Color transferring consists of two major categories: colorizing grayscale images and recoloring colored images. The literature contains a few color transfer methods that rely on some standard color spaces. In this paper, taking advantages of the principal component analysis (PCA), we propose a unifying framework for both mentioned problems. The experimental results show the efficiency of the proposed method. The performance comparison of the proposed method is also given.
© 2006 Elsevier Inc. All rights reserved.

Keywords: Color image processing; Colorizing; Color transfer; Principle component analysis

1. Introduction

Color transfer refers to the category of methods designed to change the color appearance of an image according to the color content of another image. The group of color transfer approaches contains two major categories of colorizing [1–7] and recoloring [8–11]. When we attempt to convert a grayscale source into a colored representation using the color information available in a reference image, the method is called colorizing. On the other hand, recoloring refers to the case where we wish to change the color appearance of a colored image to pretend another image's color content.

Fig. 1 shows an example of the recoloring and colorizing processes. In this figure, Fig. 1b shows the attempt to change the color of the red pepper into violet. Also, Fig. 1d shows the colorized version of the grayscale image shown in Fig. 1c.

Fig. 2 illustrates the flowchart of a typical color transfer process. It is worth to mention that different researchers use different terms to name the images taking part in this process. Here, we call the image from which the color information is extracted as the reference image, while the image on which these color information is applied is called the source image. Finally, the source image with the color information added to it is called the destination image. In the system shown in Fig. 2, a few color categories are extracted from the reference image. Also, a mechanism is designed to generate the corresponding color vector for a given grayscale value given that it belongs to one of the color categories. Consequently, the heart of the system is the classifier which decides the associated color category for each pixel in the source image. Using this methodology, we will briefly review the available color transfer literature. In this paper, after a brief review of the available color transfer approaches, we focus on the common points of all of them. Basically, we show that one of the main differences between the approaches discussed in the available literature is over the choice of the best color space in which the transformation is performed. Then, we refer to the available theoretical results that show that none of the fixed color spaces, including those which are used in the available color transfer approaches, is able to decorrelate color components. Having known that the first step in color

* Corresponding author. Fax: +98 21 6601 9246.
E-mail addresses: abadpour@math.sharif.edu (A. Abadpour), skasaei@sharif.edu (S. Kasaei).

1047-3203/$ - see front matter © 2006 Elsevier Inc. All rights reserved.
doi:10.1016/j.jvcir.2006.08.001

Fig. 1. Results of the proposed color transform methods. (a) Original color image. (b) Recolorized image. (c) Original grayscale image. (d) Colorized image. (For interpretation of the references to color in this figure legend, the reader is referred to the web version of this paper.)

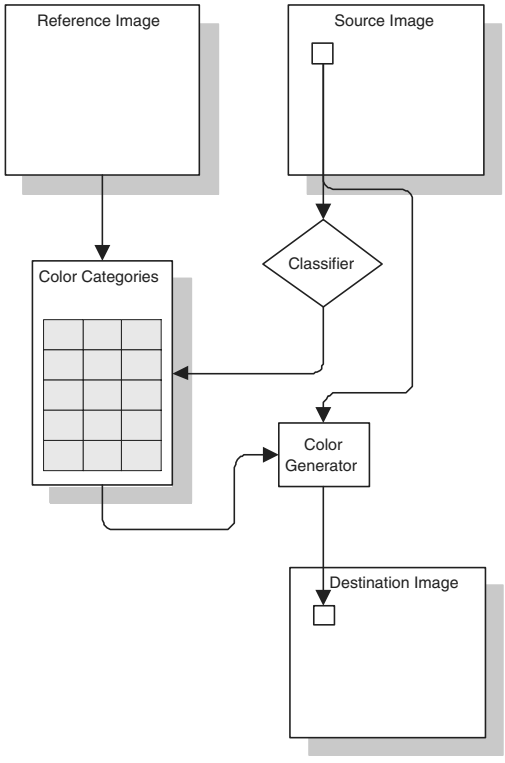

Fig. 2. A typical color transfer system.

transfer stage is to acquire these components, we focus on the mathematics of applying the PCA-based transformation approach. This path is selected because the theory predicts that the transformation given by the PCA is theoretically and practically able to do the decorrelation task. Consequently, this paper includes the methods to transfer the color between images based on the components given by the PCA.

The rest of this paper is organized as follows. First, Sections 1.1 and 1.2 briefly review the available color transfer literature. Then, Section 2 discuses the available results for the application of PCA to color image processing. These ideas are used in Section 3 to introduce the proposed methods. Section 4 contains the experimental results and discussions and finally, Section 5 concludes the paper.

1.1. Related literature on grayscale image colorizing

Colorizing refers to assigning a 3-D color vector to a 1-D luminance or brightness realization. Thus, the problem is absolutely ill-posed with no exact solution. The simplest solution ever raised for the colorizing problem is the pseudocoloring first introduced by Gonzalez and Wintz [7]. Using a set of 255 manually selected color samples as the color reference, their method is not concerned with producing real-looking images.

In an innovative work, Welsh et al. [1] applied the $\ell\alpha\beta$ color space designed by Ruderman et al. [12] to the colorizing process. Their method basically searches for similar ℓ values in the reference image and assigns the respective α and β values to the source image pixels. The method is designed for images in which "corresponding color regions

between the two images also correspond in luminance values'' [1]. Elapsing 15 s to 4 min, their method fails for images which contain blurred edges such as faces. Although, the paper concludes that the approach ''is not claimed to work on most images'' [1], the method is used by many other researchers [2,3,6].

In a different approach, Horiuchi and Hirano [4], Horiuchi [13], and Levin et al. [5], used an optimization framework for colorizing. This way, Horiuchi et al. [4] used a set of seed points and their respective color vectors in the *RGB* format and used a *YUV*-based classification. Then, the method in [4] interpolated the *RGB* coordinates given that in each pixel the produced color vector must satisfy the initial Y value in the grayscale image. The paper reports the elapsed time as a few seconds [4]. In a more deliberated approach, Levin et al. [5] used a quadratic objective function-based optimization method to interpolate the U and V components of the *YUV* color space over the entire image using a set of color scribble lines. That method elapses 15 s in average-sized images.

There is also a literature for colorizing cartoon images [14,15] that assumes that the background is a static image and all objects constitute well-visible outlines. This approach is completely different from colorizing real photographs and paintings and thus is not discussed here.

1.2. Related work on recoloring color images

Reinhard et al. [8] are perhaps the first team to work on color transfer. They described their core strategy as choosing a suitable color space for the color generator which works in an statistical framework. Using the $\ell\alpha\beta$ color space their first approach was to linearly map the pixels from the stochastic distribution of the source image to that of the reference image. In that scheme, the whole image is defined as a single color category, so there is no color classifier presented. As the paper describes, the performance of the method depends on the similarity of the images [8]. To overcome this shortcoming, Reinhard et al. proposed to use swatches. Then, for the given color vector the classifier computes its fuzzy membership to each color category using the inverse Euclidean distance. Then, a linear color transformation is applied within each class. Then, Yin et al. [9] used the same idea in the *HSI* color space specifically for face images.

Chang et al. [10] worked on color transfer from a colored painting to a colored photograph. They used an early work by Berlin and Kay [16] which examines 98 languages from several families and report that there are regularities in the number of basic colors and their spread on the color space. Chang et al.'s work [10], which is implemented entirely in the CIE–La^*b^* color space, uses later works that defines the spread of these categories. Basically, that method linearly transforms the source vectors on the reference images using the predefined classes.

Greenfield and House designed a method for color transfer between color paintings using the $\ell\alpha\beta$ color space [11]. They organized the source and the reference images into a pyramid to produce a palette for each image. Emphasizing that their primary focus was not making an intelligent pallet association process they proposed a simple association method. Each pallet color serves as a color category and the color generator transfers the α and β components. Then, a color correction process to compensate for ℓ variations is performed. While the method by Greenfield et al. [11] suffers from the same problem of the Chang et al.'s approach [10] (because of leaving no room for user intervention) they used the spatial distribution of the color vectors more professionally. One of the main shortcoming of the method by Chang et al. [10] is their assumptions for pallet association.

Table 1
Standard color spaces used in different color transfer approaches

Work	Color space
Welsh et al. [1], Reinhard et al. [8], Greenfield et al. [11]	$\ell\alpha\beta$
Horiuchi et al. [4], Levin et al. [5]	*YUV*
Chang et al. [10]	CIE–La^*b^*
Yin et al. [9]	*RGB*

Neglecting the details, all of the available color transfer methods (containing both colorization and recoloring approaches), use the same assumption that there exists an standard color space that performs well in decorrelating the color components (see Table 1). It is shown in different works (*e.g.*, [17–19]) that none of the standard color spaces are successful in giving a decorrelated representation of the color vectors in an unconditional imaging framework for classification or the kinds of direct manipulations mentioned here. Also, the Euclidean distance-based classifiers used by Reinhard et al. [8] and Welsh et al. [1] has been shown to result in spurious results [20].

2. Previous work on PCA-based color processing

In 1988, Klinker et al. presented a novel approach for measuring the highlights in color images [21]. There, they developed a proper model for the reflected light from an arbitrary point of a dielectric object. In 1990, they applied their approach to color image understanding [22]. However, more than a decade passed since the idea was successfully incorporated into a practical algorithm. In 2003, without being seriously involved in the theoretical aspects, Cheng and Hsia used the principal component analysis (PCA) for color image processing [23]. Then, in 2004, Nikolaev and Nikolayev started the work again from the theory and showed that the PCA is a proper tool for color image processing [24]. The next necessary step was introduced in the early 1991, when Turk and Pentland proposed their eigenface method [25]. There, they developed a novel idea which connected the eigenproblems in the color domain with the ones in the spatial domain. Although, there is this rich theoretical background for the linear local models of color constancy, it is quite common to see research procedures which are based on the old color space paradigm, even in 2006.

Color is one of the most important tools for object discrimination by human observers, but it is overlooked in the past [26]. Discarding the intrinsic characteristics of color images (as vector geometries [27]), many researchers have assumed color images as parallel grayscale images (*e.g.*, see [28–31]). It has been shown that the PCA is an appropriate vectorial descriptor for color images [32,20,23]. In [32], the authors proposed to use the error made by neglecting the two least important principal components (the second and the third) as a likelihood measure for color vectors. As such, the linear partial reconstruction error (LPRE) distance of vector $\vec{\mathbf{c}}$ to cluster r is defined as:

$$\tau_r(\vec{\mathbf{c}}) = \|\vec{\mathbf{v}}^{\mathrm{T}}(\vec{\mathbf{c}} - \vec{\eta})\vec{\mathbf{v}} - (\vec{\mathbf{c}} - \vec{\eta})\|, \tag{1}$$

where $\vec{\eta}$ and $\vec{\mathbf{v}}$ denote the expectation vector and the direction of the first principal component of cluster r. Also, $\|\vec{\mathbf{x}}\|$ is the normalized L_1 norm defined as $\|\vec{\mathbf{x}}\| = \frac{1}{3}\sum_{i=1}^{3}|x_i|$. In [32], the authors proposed the normalized LPRE homogeneity measure as

$$\tilde{\tau}_r(\vec{\mathbf{c}}) = \frac{\tau_r(\vec{\mathbf{c}})}{E_{\vec{\mathbf{x}}\in c}\{\tau_r(\vec{\mathbf{x}})\}}. \tag{2}$$

It is shown that $E_{\vec{\mathbf{x}}\in c}\{\tau_r(\vec{\mathbf{x}})\}$ is a proper homogeneity criterion for usages such as tree decomposition [33], and $\tilde{\tau}_r(\vec{\mathbf{c}})$ serves as a perfect likelihood measure for color images [20]. The comparison of the LPRE-based homogeneity criterion and likelihood measure with the Euclidean and the Mahalanobis-based approaches has shown its absolute superiority over both of them [20]. Also, it is shown that the L_1 norm used in (1) may be converted to the L_2 norm [20].

Note that $\tilde{\tau}_r(\vec{\mathbf{c}})$ gives lower values to the color vectors *similar* to those that exist in r. Thus, a function is needed to map $[-1,1]$ into $[1, 1-\varepsilon]$ and $[-\infty,-1]\cup[1,\infty]$ into $[1-\varepsilon, 0]$ to give conventional fuzzy membership values. In [20], the authors proposed to use a manipulated form of the well-known low-pass Butterworth filter for the sake of simplicity and control, as:

$$B_{\alpha,\beta}(x) = \left(1 + \left(\frac{x}{\tau_{\alpha,\beta}}\right)^{2N_{\alpha,\beta}}\right)^{-\frac{1}{2}}, \tag{3}$$

where, $N_{\alpha,\beta}$ and $\tau_{\alpha,\beta}$ are defined as:

$$N_{\alpha,\beta} = \mathrm{rnd}\left(\log_2\left(\frac{\alpha\sqrt{1-\beta^2}}{\beta\sqrt{1-\alpha^2}}\right)\right), \tag{4}$$

$$\tau_{\alpha,\beta} = \alpha^{\frac{1}{N_{\alpha,\beta}}}\left(1-\alpha^2\right)^{-\frac{1}{2N_{\alpha,\beta}}}. \tag{5}$$

Here, $\mathrm{rnd}(x)$ denotes the nearest integer value to x. The function $B_{\alpha,\beta}(x)$ is designed such that it satisfies $B_{\alpha,\beta}(1) = \alpha$ and $B_{\alpha,\beta}(2) = \beta$. Selecting a large member of $]0,1[$ as the α value and a small member of $]0,\alpha[$ as the β value, leads to a desired fuzzyfication. Note that the above definition of membership functions is in contrast with the general selection of the Gaussian functions. Fig. 3 shows the typical shape of the membership function with the two parameters

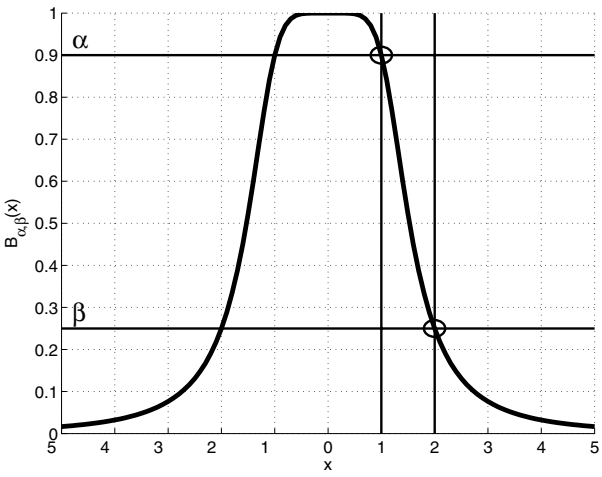

Fig. 3. Typical shape of the proposed membership function and the related α and β parameters.

α and β highlighted on it. Fig. 4 shows the log-magnitude of the membership function ($B_{\alpha,\beta}$) for different values of α and β. While larger values of β increase the domain of the typical members (those with large likelihood values) the function has an area of almost-one values for the interior points of the cluster controlled by α. This situation does not happen with the Gaussian function, in which one must increase the domain of better members (by increasing σ) leading to an overall increase of membership values. Also, the sharp transition between the points $(1,\alpha)$ and $(2,\beta)$, which enables the crisp classification of points in the proposed membership functions, does not exist in the Gaussian function. Using the definition of the normalized reconstruction error in (1) and the reformulated Butterworth function in (3), an image is fuzzificated regarding the query region r by using $B_{\alpha,\beta}(\tilde{\tau}_r(\vec{\mathbf{c}}))$. Note that the points in r (and points similar to them in the color sense) are mostly giving membership values in the range of $[1,\alpha]$. The color vectors that are not similar to those existing in r are ranked with poor values.

The comprehensive investigation of the above fuzzification method in [20] has shown its performance for processing of color images. The values of α and β control the shape of the membership function and are left to the user to tune the function to well fit the constraints of the problem in hand. As for all $x \in [0,1]$, $B_{\alpha,\beta}(x)$ must gain high levels of membership, in [20] the authors proposed to set $\alpha = 0.99$. Now, By tuning the β parameter, one can easily control the distribution of the membership function. This leads to the single parameter fuzzification function defined as:

$$h_{r,\beta}(\vec{\mathbf{c}}) = B_{0.99,\beta}(\tilde{\tau}_r(\vec{\mathbf{c}})). \tag{6}$$

3. Proposed methods

In this section, we will first propose a novel dimension reduction technique for color images in Section 3.1. The dimension reduction method and the color model which

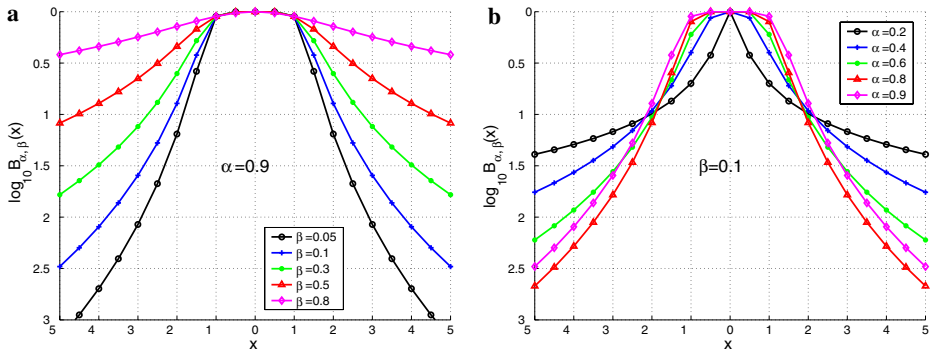

Fig. 4. Log-magnitude of the membership function ($B_{\alpha,\beta}$). (a) $\alpha = 0.9$ with different values of β. (b) $\beta = 0.1$ with different values of α.

is based on it are used in Sections 3.2 and 3.3 to propose a colorizing and a recoloring method, respectively. In all formulas, the variables indexed as x_1, x_2, and x'_1 belong to the source, the reference, and the destination images, respectively.

3.1. Color space dimension reduction for color images

Consider the color cluster r and the color vector $\vec{\mathbf{c}}$ belonging to r. Assume that $\vec{\eta}$ is the expectation vector of the members of r. Here, the expectation vector is defined as the average of all the vectors in r. Also, $\mathbf{C}$ is the matrix including the eigenvectors of the covariance matrix of r (as its columns sorted according to the eigenvalues in a descending fashion), and $\vec{\mathbf{v}}_\mathbf{i}$ is the direction of the ith principal component of r, ($i = 1, 2,$ and 3). Thus, $\vec{\mathbf{v}}_\mathbf{i}$ is the ith column of $\mathbf{C}$. The color vector $\vec{\mathbf{c}}$ in the PCA coordinates is computed as:

$$\vec{\mathbf{c}}_\mathbf{p} = \begin{pmatrix} \mathrm{pc}_1 \\ \mathrm{pc}_2 \\ \mathrm{pc}_3 \end{pmatrix} = \mathbf{C}^{-1}(\vec{\mathbf{c}} - \vec{\eta}). \tag{7}$$

Here, pc_i is the ith principal component of the color vector $\vec{\mathbf{c}}$. Although, $\vec{\mathbf{c}}_\mathbf{p}$ is a 3-D vector, the theory states that pc_1 is sufficient to perform classification tasks on $\vec{\mathbf{c}}$ (see Section 2). As $\vec{\mathbf{v}}_\mathbf{1}$ is the first column of the orthonormal matrix $\mathbf{C}$, pc_1 is independently computed as:

$$\mathrm{pc}_1 = \vec{\mathbf{v}}_\mathbf{1}^{\mathrm{T}}(\vec{\mathbf{c}} - \vec{\eta}). \tag{8}$$

Having pc_1, we can partially reconstruct the color vector $\vec{\mathbf{c}}$ as $\vec{\mathbf{c}}_\circ$ using

$$\vec{\mathbf{c}}_\circ = \mathrm{pc}_1\vec{\mathbf{v}}_\mathbf{1} + \vec{\eta} = [\vec{\mathbf{v}}_1^{\mathrm{T}}(\vec{\mathbf{c}} - \vec{\eta})]\vec{\mathbf{v}} + \vec{\eta}. \tag{9}$$

The performance of PCA for color vectors relies on the fact that color clusters in the color images of the nature can be estimated using cylindrical shapes, represented by an axis and a center [34]. Thus, it is reasonable to expect that $\vec{\mathbf{c}}_\circ$ is a proper estimation of the original vector $\vec{\mathbf{c}}$. The measure used for the suitability of this dimension reduction scheme is the subjective appearance of the result along with the PSNR. The experimental results show the efficiency of this scheme. In fact, it enables us to convert a 3-D homogeneous swatch in a color image into a 1-D representation, reaching a dimension reduction of 2. This is further discussed in Section 4.

Now, we will turn back to (7) to analytically estimate the energy compaction of the PCA for color images. Assume that the three components of $\vec{\mathbf{c}}$ are defined as c_1, c_2, and c_3. We will first prove that

$$\sigma^2_{c_1} + \sigma^2_{c_2} + \sigma^2_{c_3} = \sigma^2_{\mathrm{pc}_1} + \sigma^2_{\mathrm{pc}_2} + \sigma^2_{\mathrm{pc}_3}. \tag{10}$$

This equality declares that the amount of the energy before and after the PCA transformation is not changed. Thus, we can think of the energy compaction of c_i and pc_i channels in the same framework. Let the element of the matrix $\mathbf{C}$ in the ith row and jth column be denoted by C_{ij}. Thus, we have

$$\mathrm{pc}_i = C_{i1}c_1 + C_{i2}c_2 + C_{i3}c_3, \tag{11}$$

and,

$$E\{\mathrm{pc}_i\} = C_{i1}E\{c_1\} + C_{i2}E\{c_2\} + C_{i3}E\{c_3\}. \tag{12}$$

So,

$$\begin{aligned}\sigma^2_{\mathrm{pc}_i} &= E\{(\mathrm{pc}_i - E\{\mathrm{pc}_i\})^2\} \\ &= \sum_{j=1}^{3} C^2_{ij}\sigma^2_{c_j} + 2\sum_{j=1}^{3}\sum_{k=1,k<j}^{3} C_{ij}C_{ik}\sigma_{c_jc_k}\end{aligned} \tag{13}$$

where, $\sigma_{c_jc_k}$ is the cross–correlation of c_j and c_k defined as:

$$\sigma_{c_jc_k} = E\{(c_j - E\{c_j\})(c_k - E\{c_k\})\}. \tag{14}$$

Computing $\sigma^2_{\mathrm{pc}_1} + \sigma^2_{\mathrm{pc}_2} + \sigma^2_{\mathrm{pc}_3}$ using (13) for values of $i = 1$, 2, and 3, we will have

$$\begin{aligned}\sum_{i=1}^{3}\sigma^2_{\mathrm{pc}_i} = \sum_{j=1}^{3}\left(\sigma^2_{c_j}\sum_{i=1}^{3}C^2_{ij}\right) + 2\sum_{j=1}^{3}\sum_{k=1,k<j}^{3}\sigma_{c_jc_k} \\ \times \sum_{i=1}^{3} C_{ij}C_{ik}.\end{aligned} \tag{15}$$

So,

$$\sum_{i=1}^{3}\sigma^2_{\mathrm{pc}_i} = \sum_{j=1}^{3}\sigma^2_{c_j}\|\vec{\mathbf{v}}_\mathbf{j}\|^2 + 2\sum_{j=1}^{3}\sum_{k=1,k<j}^{3}\sigma_{c_jc_k}\vec{\mathbf{v}}_\mathbf{j}^{\mathrm{T}}\vec{\mathbf{v}}_\mathbf{k}. \tag{16}$$

As $\mathbf{C}$ is an orthonormal matrix, we have the normality ($\|\vec{\mathbf{v}}_\mathbf{i}\|^2 = 1$) and the orthogonality ($\vec{\mathbf{v}}_\mathbf{j}^{\mathrm{T}}\vec{\mathbf{v}}_\mathbf{k} = 0$) constraints

on its columns. Thus, equation (16) changes to equation (10), proving the claim.

The equality of the sum of the standard deviations makes it reasonable to define the energy ratio of κ_x as:

$$\kappa_x = \frac{\sigma_x^2}{\sigma_{c_1}^2 + \sigma_{c_2}^2 + \sigma_{c_3}^2}. \tag{17}$$

Here, x is one of the color components of c_1, c_2, c_3, pc_1, pc_2, or pc_3. Note that

$$\kappa_{c_1} + \kappa_{c_2} + \kappa_{c_3} = \kappa_{\mathrm{pc}_1} + \kappa_{\mathrm{pc}_2} + \kappa_{\mathrm{pc}_3} = 1. \tag{18}$$

The larger the κ_x, the more important we expect the corresponding channel to be. We expect $\kappa_{\mathrm{pc}_1} \gg \kappa_{\mathrm{pc}_2} \gg \kappa_{\mathrm{pc}_3}$ to make it reasonable to eliminate pc_2 and pc_3 while saving the image quality.

3.2. Proposed grayscale image colorizing

The proposed method for grayscale image colorization does not depend on any particular color space and works using a linear definition for the achromatic norm defined below. In Section 3.2.1, some considerations for a suitable norm function are discussed. The proposed method is then presented in Section 3.2.2.

3.2.1. Color to grayscale transformation

Many types of illumination measures are discussed in the literature (also called brightness and intensity), with different meanings and aims (*e.g.*, see [35–40]). To be general, we call such a measure the achromatic norm of a color vector or simply its norm. To use the linear algebra concepts we limit our work to linear norm functions generally shown as:

$$\langle \vec{\mathbf{v}} \rangle = \vec{\mathbf{N}}^{\mathrm{T}} \vec{\mathbf{v}} \tag{19}$$

where the vector $\vec{\mathbf{N}}$ is selected in the way that it satisfies the condition $\langle \vec{\mathbf{1}} \rangle = 1$. The above defined norm function satisfies two simple but important conditions of

$$\langle \alpha \vec{\mathbf{v_1}} + \vec{\mathbf{v_2}} \rangle = \alpha \langle \vec{\mathbf{v_1}} \rangle + \langle \vec{\mathbf{v_2}} \rangle, \tag{20}$$

$$E\{\langle \vec{\mathbf{x}} \rangle\} = \langle E\{\vec{\mathbf{x}}\} \rangle. \tag{21}$$

3.2.2. Grayscale image colorizing

As the transformation from a *3*-D color vector to a single intensity number is irreversible, there can be many, extremely, different colors with the same appearance in the grayscale image. One method to distinguish such spurious points is to use some neighborhood information; as proposed in Welsh et al.'s method [1]. Their method is based on an unprovable assumption that the color regions of the same object lie in the same range of intensity. Having in mind the desperate performance that they have reported, along with the wide range of images in which the method fails (containing the major category of face images) the need for an efficient colorizing method arises. Furthermore, they combine the two segmentation stages for the reference and the source images, while these are in entirely different domains (one is a color image whilst the other essentially is a grayscale one). To overcome the shortcomings of Welsh et al.'s work [1], here we separate the color extraction and segmentation processes. This way we are only addressing the color reproduction stage. It is obvious that the segmentation phase has a very serious effect on the results. The problem we work on here is, given that the segmentation is done which colorizing process performs better.

Here, we propose a colorizing approach which asks the user for an indexed map which for each pixel gives the corresponding class to which it belongs. Then, for each class, the user gives a homogeneous color swatch as the reference color from which the color information is extracted and applied to the respective segments of the source image. The process runs over all swatches to produce the destination image. Fig. 5 shows a sample set of inputs to the proposed colorizing method along with the result. Fig. 5a shows the source image categorized into two classes of leaves and bark as shown in Fig. 5b. Fig. 5c illustrates the reference image and the two representative swatches and Fig. 5d shows the result of the proposed colorizing method. As discussed in Section 3.1, the expectation vector and the direction of the first principal component of a given cluster are proper descriptors for modeling the color content. Having a grayscale pixel and the above color descriptors, we propose to generate a proper color vector using the color descriptors of the reference swatch. As there exists no objective criterion for comparing different colorizing algorithms in the literature, here we propose three conditions to be met by a perfect colorizing process. First, it is reasonable to expect a colorizing process to not to alter the original grayscale information of the image. Thus, For the source image I_1, the reference image I_2, and the destination image I'_1, we expect the grayscale version of I'_1 to be identical to I_1. As the second and the third conditions, we force the colorizing method to embed the same color information extracted from the reference image into the destination image. The transfer should be designed in the way that using the destination as the reference image for another colorizing task results the same as using the original reference image. We formulate the second and the third conditions as $\vec{\eta}'_1 \| \vec{\eta}_2$ and $\vec{\mathbf{v}}_1' = \vec{\mathbf{v}}_2$, respectively. The first condition forces the expectation vector of the colorized image to be parallel to the expectation vector of the reference image and the third condition limits the direction of its first principal component to be identical to that of the reference image. Note that by expectation vector we mean the vector corresponding to a single segment or a single swatch. Note that nothing is said about segments in a color image containing a set of non-homogeneous color vectors. We will come back to these conditions and discuss them more later.

In this work, we propose a new category of colorizing methods that generate the color vector corresponding to the grayscale c_1 as a function of η_1, $\vec{\eta}_2$, and $\vec{\mathbf{v}}_2$. These

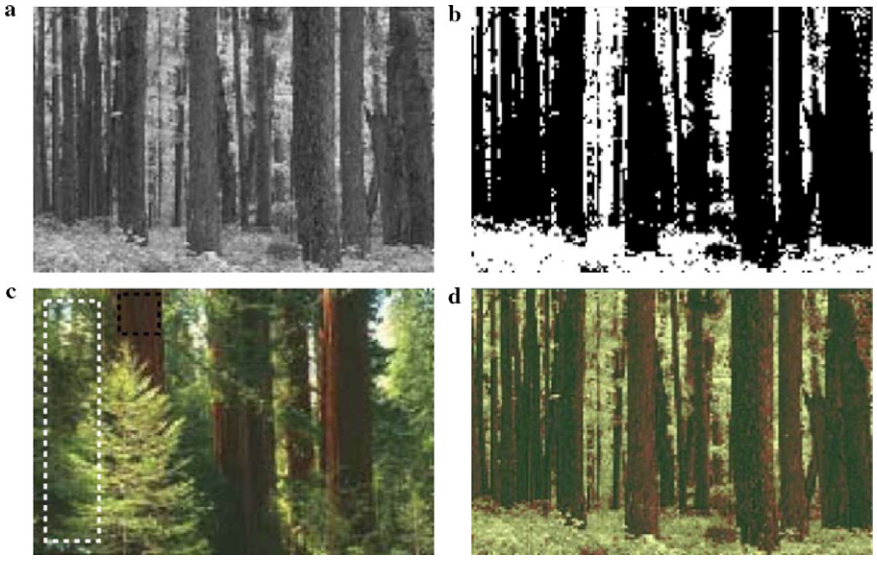

Fig. 5. Typical input and output of the proposed colorizing method. (a) Source image. (b) Index map. (c) Reference image and the representative swatches. (d) Resulting colorized image. (For interpretation of the references to color in this figure legend, the reader is referred to the web version of this paper.)

notions correspond to the expectation of the grayscale values in the source image, the expectation vector, and the direction of the first principal component of the associated color cluster in the reference image, respectively. Note that, using the segmentation information given by the user, all variables relate to the same cluster to which the pixel with the grayscale value of c_1 in the source image is related. The color vector relating to c_1 is generated as:

$$\vec{\mathbf{c}}_1' = \Phi_{\eta_1,\vec{\eta}_2,\vec{\mathbf{v}}_2}(c_1). \tag{22}$$

Here, Φ should satisfy the above three constraints. Many different formulations are designed and implemented by the authors. The two most appropriate are

$$\vec{\mathbf{c}}_1' = \vec{\eta}_2 + (c_1 - \langle\vec{\eta}_2\rangle)\frac{\vec{\mathbf{v}}_2}{\langle\vec{\mathbf{v}}_2\rangle}, \tag{23}$$

$$\vec{\mathbf{c}}_1' = \frac{\eta_1}{\langle\vec{\eta}_2\rangle}\vec{\eta}_2 + (c_1 - \eta_1)\frac{\vec{\mathbf{v}}_2}{\langle\vec{\mathbf{v}}_2\rangle}. \tag{24}$$

Investigating the fulfillment of the first condition in (23) we have

$$\langle\vec{\mathbf{c}}_1'\rangle = \langle\vec{\eta}_2\rangle + (c_1 - \langle\vec{\eta}_2\rangle)\frac{\langle\vec{\mathbf{v}}_2\rangle}{\langle\vec{\mathbf{v}}_2\rangle} = c_1, \tag{25}$$

which means that turning the destination vector back to the grayscale domain reverts it to the same grayscale value as it was in the source image. Also, we have

$$\vec{\eta}_1' = E\{\vec{\mathbf{c}}_1'\} = \vec{\eta}_2 + (\eta_1 - \langle\vec{\eta}_2\rangle)\frac{\vec{\mathbf{v}}_2}{\langle\vec{\mathbf{v}}_2\rangle}, \tag{26}$$

which is not parallel to $\vec{\eta}_2$, contradicting the second condition. To investigate the third condition, we compute the covariance matrix of $\vec{\mathbf{c}}_1'$ as:

$$\mathbf{C}_1' = E\{(\vec{\mathbf{c}}_1' - \vec{\eta}_1')(\vec{c}_1' - \vec{\eta}_1')^{\mathrm{T}}\}. \tag{27}$$

Note that

$$\begin{aligned}\vec{\mathbf{c}}_1' - \vec{\eta}_1' &= \vec{\eta}_2 + (c_1 - \langle\vec{\eta}_2\rangle)\frac{\vec{\mathbf{v}}_2}{\langle\vec{\mathbf{v}}_2\rangle} - \vec{\eta}_2 - (E\{c_1\} - \langle\vec{\eta}_2\rangle)\frac{\vec{\mathbf{v}}_2}{\langle\vec{\mathbf{v}}_2\rangle} \\ &= (c_1 - \eta_1)\frac{\vec{\mathbf{v}}_2}{\langle\vec{\mathbf{v}}_2\rangle}.\end{aligned} \tag{28}$$

Substituting (28) in (27) gives

$$\mathbf{C}_1' = \frac{\mathbf{E}\{(c_1 - \eta_1)^2\}}{\langle\vec{\mathbf{v}}_2\rangle^2}\vec{\mathbf{v}}_2\vec{\mathbf{v}}_2^{\mathrm{T}} = \frac{\sigma_{c_1}^2}{\langle\vec{\mathbf{v}}_2\rangle^2}\vec{\mathbf{v}}_2\vec{\mathbf{v}}_2^{\mathrm{T}}. \tag{29}$$

Also, we have

$$\frac{\sigma_{c_1}^2}{\langle\vec{\mathbf{v}}_2\rangle^2}(\vec{\mathbf{v}}_2\vec{\mathbf{v}}_2^{\mathrm{T}})\vec{\mathbf{v}}_2 = \frac{\sigma_{c_1}^2\|\vec{\mathbf{v}}_2\|^2}{\langle\vec{\mathbf{v}}_2\rangle^2}\vec{\mathbf{v}}_2 = \frac{\sigma_{c_1}^2}{\langle\vec{v}_2\rangle^2}\vec{\mathbf{v}}_2, \tag{30}$$

which means that the vector $\vec{\mathbf{v}}_2$ is an eigenvector of matrix $\mathbf{C}_1'$. As the rank of the 3×3 matrix $\mathbf{C}_1'$ is unity, $\vec{\mathbf{v}}_2$ is its only eigenvector. Thus, the direction of the first principal component of $\vec{\mathbf{c}}_1'$ is the same as the ones relating to the reference image (fulfilling the third condition). Hence, (23) satisfies the first and the third criteria while failing the second.

Returning to the solution proposed in (24) we have

$$\langle\vec{\mathbf{c}}_1'\rangle = \frac{\eta_1}{\langle\vec{\eta}_2\rangle}\langle\vec{\eta}_2\rangle + (c_1 - \eta_1)\frac{\langle\vec{\mathbf{v}}_2\rangle}{\langle\vec{\mathbf{v}}_2\rangle} = c_1 \tag{31}$$

meaning that turning back the destination image to the grayscale domain reverts it back to the source image. The second criterion uses $E\{\vec{\mathbf{c}}_1'\}$, where we have

$$E\{\vec{\mathbf{c}}_1'\} = \frac{\eta_1}{\langle\vec{\eta}_2\rangle}\vec{\eta}_2 + (\eta_1 - \eta_1)\frac{\vec{\mathbf{v}}_2}{\langle\vec{v}_2\rangle} = \frac{\eta_1}{\langle\vec{\eta}_2\rangle}\vec{\eta}_2 \Big\| \vec{\eta}_2 \tag{32}$$

complying with the second criterion. For the third criterion, we compute the covariance matrix of $\vec{\mathbf{c}}_1'$ as:

$$\mathbf{C}_1' = E\{(\vec{\mathbf{c}}_1' - \vec{\eta}_1')(\vec{\mathbf{c}}_1' - \vec{\eta}_1')^{\mathrm{T}}\}. \tag{33}$$

Also, we have

$$\vec{\mathbf{c}}_1' - \vec{\eta}_1' = \frac{\eta_1}{\langle \vec{\eta}_2 \rangle}\vec{\eta}_2 + (c_1 - \eta_1)\frac{\vec{\mathbf{v}}_2}{\langle \vec{v}_2 \rangle} - \frac{\eta_1}{\langle \vec{\eta}_2 \rangle}\vec{\eta}_2 = (c_1 - \eta_1)\frac{\vec{\mathbf{v}}_2}{\langle \vec{v}_2 \rangle}, \quad (34)$$

which results like (29) proving that the third criterion is also fulfilled. Thus, the formula in (24) complies with all three criteria.

Considering the computation costs, both (23) and (24) cost three subtractions, three additions and three multiplications for each pixel in the colorization stage.

As the method by Welsh et al. [1] is adopted in many other works, a subjective test is performed to compare the performance of that method with the proposed methods. To do so, 26 persons aged 17–27 were asked to reorder the three images resulting from Welsh's approach [1] and the results of the methods proposed in (23) and (24) in terms of goodness scales [41] (Table 3). The subjects were unaware of the algorithms but were literate people. Neither the source image nor the reference images were exposed to the subjects and they were able to scroll the monitor in order to watch any of the three images at any time they intended to see, but not zooming into them. The images were shown in a randomly ordered fashion and no timing threshold was set. The answers were given as strings containing "1","2", and "3" along with "," and "/". For example, "1/2, 3" denoted that the first image is the best, and the second and the third ones look the same in the next place. Subjects were not allowed to discuss the results with each other. The orders were changed to scores in the range of $[0, \ldots, 3]$ and subsequently an statistical analysis was preformed on them. Also, human perception was measured by means of impairment (Table 2) and goodness (Table 3) scales [41]. The results are discussed in Section 4.3.

3.3. Proposed color transfer between images

Table 2
Impairment scales [41]

Scale	Meaning
1	Not noticeable
2	Just noticeable
3	Definitely noticeable but only slight impairments
4	Impairment not objectionable
5	Somewhat objectionable
6	Definitely objectionable
7	Extremely objectionable

Table 3
Goodness scales [41]

Scale	Meaning
5	Excellent
4	Good
3	Fair
2	Poor
1	Unsatisfactory

User contribution in the proposed color image recoloring method is limited to selecting a few corresponding swatches in the reference and the source images, along with tuning a one-parameter membership function. In Section 3.3.1, we first propose a framework to transfer the color content of a homogeneous swatch to another homogeneous swatch and discuss the mathematical perspective. We call this intermediate stage single-swatch recoloring. Then, using the fuzzification method (discussed in Section 2) we generalize the method for recoloring the entire image using a set of corresponding homogeneous swatches. Notations in this section are the same as those used in Section 3.2.

Fig. 6 shows a sample result of the proposed recoloring method. Figs. 6a and b show the source and the reference images with the overlayed swatches. Figs. 6c and d illustrate the fuzzy membership of the pixels of the source images to the first and the second swatches of the source image, respectively. Figs. 6e and f illustrate the results of single swatch recoloring. Note that in Fig. 6e the flower color has changed to the desired one, while the leaves are recolorized perfectly in Fig. 6f. Finally, Fig. 6g shows the final result of the pro-

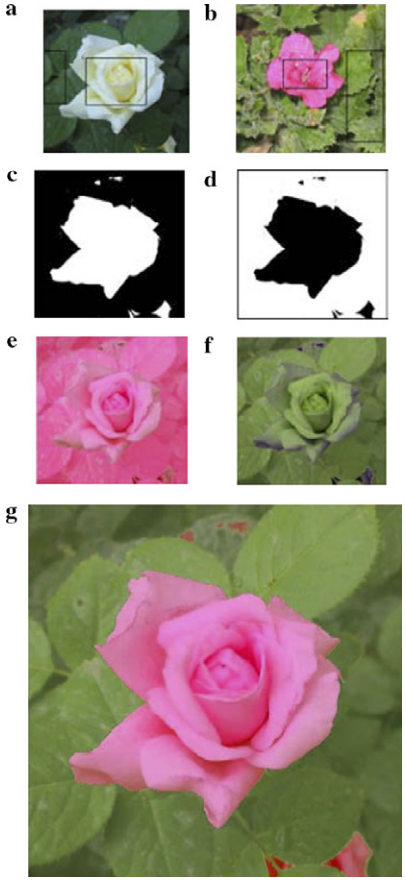

Fig. 6. Sample results of proposed recoloring method. (a) Source Image and the overlayed swatches. (b) Reference image and the overlayed swatches. (c) Fuzzy membership of source pixels to the flower group. (d) Fuzzy membership of source pixels to the leaf group. (e) Results of the proposed single-swatch recoloring according to the flower swatches. (f) Results of the proposed single-swatch recoloring according to the leaf swatches. (g) Final result. (For interpretation of the references to color in this figure legend, the reader is referred to the web version of this paper.)

posed method, incorporating both the single-swatch recoloring results and the fuzzy membership values.

3.3.1. Single-swatch recoloring

Assume that the source image I_1 and the reference image I_2 are both containing homogeneous vectors. This assumption is the same as Reinhard et al.'s first recoloring method [8]. As discussed in Section 3.1 and Section 3.2 and also in [42,43], the PCA framework is a reliable tool to model color distribution of homogeneous swatches. Thus, here we use a linear method to propose the single-swatch recoloring method.

Assume that the vectors $\vec{\eta}_1$, $\vec{\eta}_2$, $\mathbf{V_1}$, and $\mathbf{V_2}$ denote the expectation vector of color information in I_1, I_2, and their corresponding PCA matrices, respectively. The PCA matrix is the one containing the eigenvectors of the respective covariance matrix as its columns sorted by the eigenvalues in a descending fashion. Note that both $\mathbf{V_1}$ and $\mathbf{V_2}$ are orthonormal matrices. Here, we propose to compute the color vector $\vec{\mathbf{c}}_1'$ as the result of recoloring the color vector $\vec{\mathbf{c}}_1$ as:

$$\vec{\mathbf{c}}_1' = \mathbf{V_2}\mathbf{V_1}^{-1}(\vec{\mathbf{c}}_1 - \vec{\eta}_1) + \vec{\eta}_2. \tag{35}$$

Now, lets investigate the properties of $\vec{\mathbf{c}}_1'$ in more details. Computing the expectation vector of I_1' (the destination image) we have

$$\vec{\eta}_1' = E\{\vec{\mathbf{c}}_1'\} = \mathbf{V_2}\mathbf{V_1}^{-1}E\{\vec{\mathbf{c}}_1 - \vec{\eta}_1\} + \vec{\eta}_2 = \vec{\eta}_2. \tag{36}$$

Note that $\mathbf{V_1}$ and $\mathbf{V_2}$ are constant matrices. Thus, the expectation vector of the destination image is identical to the expectation vector of the reference image. For $\mathbf{C}_1'$ (the covariance matrix of I_1') we have

$$\mathbf{C}_1' = E\left\{(\vec{\mathbf{c}}_1' - \vec{\eta}_1')(\vec{\mathbf{c}}_1' - \vec{\eta}_1')^{\mathrm{T}}\right\}. \tag{37}$$

Also, we have

$$\vec{\mathbf{c}}_1' - \vec{\eta}_1' = \mathbf{V_2}\mathbf{V_1}^{-1}(\vec{\mathbf{c}}_1 - \vec{\eta}_1). \tag{38}$$

Substituting (38) in (37) results in

$$\begin{aligned}\mathbf{C}_1' &= E\{\mathbf{V_2}\mathbf{V_1}^{-1}(\vec{c}_1 - \vec{\eta}_1)(\mathbf{V_2}\mathbf{V_1}^{-1}(\vec{c}_1 - \vec{\eta}_1))^{\mathrm{T}}\}\\ &= E\{\mathbf{V_2}\mathbf{V_1}^{-1}(\vec{\mathbf{c}}_1 - \vec{\eta}_1)(\vec{\mathbf{c}}_1 - \vec{\eta}_1)^{\mathrm{T}}\mathbf{V_1}\mathbf{V_2}^{-1}\}\\ &= \mathbf{V_2}\mathbf{V_1}^{-1}\mathbf{C_1}\mathbf{V_1}\mathbf{V_2}^{-1}.\end{aligned} \tag{39}$$

Here, $\mathbf{C_1}$ is the covariance matrix of I_1. Assume that $\vec{\mathbf{v}}$ is the eigenvector of $\mathbf{C_1}$ corresponding to the eigenvalue of λ. Thus, we have $\mathbf{C_1}\vec{\mathbf{v}} = \lambda\vec{\mathbf{v}}$. Now, considering

$$\begin{aligned}\mathbf{C}_1'\mathbf{V_2}\mathbf{V_1}^{-1}\vec{\mathbf{v}} &= \mathbf{V_2}\mathbf{V_1}^{-1}\mathbf{C_1}\mathbf{V_1}\mathbf{V_2}^{-1}\mathbf{V_2}\mathbf{V_1}^{-1}\vec{\mathbf{v}} = \mathbf{V_2}\mathbf{V_1}^{-1}\mathbf{C_1}\vec{\mathbf{v}}\\ &= \lambda\mathbf{V_2}\mathbf{V_1}^{-1}\vec{\mathbf{v}}\end{aligned} \tag{40}$$

setting

$$\vec{\mathbf{u}} = \mathbf{V_2}\mathbf{V_1}^{-1}\vec{\mathbf{v}} \tag{41}$$

in (40), we have $\vec{\mathbf{c}}_1'\vec{\mathbf{u}} = \lambda\vec{\mathbf{u}}$. Thus, $\vec{\mathbf{u}}$ is the eigenvector of $\mathbf{C}_1'$ with the same eigenvalue of λ. Hence, the eigenvectors of $\mathbf{C}_1'$ are computed from those of $\mathbf{C_1}$ using (41). Note that their orders remains identical. This proves that $\mathbf{V}_1'$ (the PCA matrix of I_1') equals

$$\mathbf{V}_1' = \mathbf{V_2}\mathbf{V_1}^{-1}\mathbf{V_1} = \mathbf{V_2}. \tag{42}$$

Eqs. (42) and (36) prove that when recoloring a source image with a reference image using the proposed method, the color models get identical. This important result has a few fascinating outcomes. First, assume that after recoloring I_1 with I_2 to have I_1', we are not satisfied with it and we want to revert it. Recoloring I_1' with the color information extracted from the original source image, the new destination image (I_1'') is computed as:

$$\begin{aligned}\vec{\mathbf{c}}_1'' &= \mathbf{V_1}\mathbf{V_2}^{-1}(\vec{c}_1' - \vec{\eta}_2) + \vec{\eta}_1\\ &= \mathbf{V_1}\mathbf{V_2}^{-1}(\mathbf{V_2}\mathbf{V_1}^{-1}(\vec{c}_1 - \vec{\eta}_1) + \vec{\eta}_2 - \vec{\eta}_2) + \vec{\eta}_1 = \vec{\mathbf{c}}_1.\end{aligned} \tag{43}$$

Thus, I_1'' is identical to the original I_1', meaning that the proposed single-swatch recoloring scheme is completely invertible.

As another property of the proposed recoloring method, consider the three images I_1, I_2, and I_3. Assume that we have performed recoloring process on I_1 using the reference image of I_2 to acquire I_1'. Also, assume that we have used I_1' as a new source image and I_3 as the reference image to compute I_2'. Also, assume eliminating the intermediate stage and recolor I_1 according to I_3 to get I_1''. Thus, we have

$$\begin{aligned}\vec{\mathbf{c}}_2' &= V_3\mathbf{V_2}^{-1}(\vec{c}_1' - \vec{\eta}_2) + \vec{\eta}_3\\ &= V_3\mathbf{V_2}^{-1}(\mathbf{V_2}\mathbf{V_1}^{-1}(\vec{c}_1 - \vec{\eta}_1) + \vec{\eta}_2 - \vec{\eta}_2) + \vec{\eta}_3\\ &= V_3\mathbf{V_1}^{-1}(\vec{c}_1 - \vec{\eta}_1) + \vec{\eta}_3,\end{aligned} \tag{44}$$

and

$$\vec{\mathbf{c}}_1'' = V_3\mathbf{V_1}^{-1}(\vec{c}_1 - \vec{\eta}_1) + \vec{\eta}_3. \tag{45}$$

Comparing (44) and (45) proves that I_1'' is identical to I_2'. Hence, the proposed single-swatch recoloring scheme is transitive.

As the final property of the prosed single-swatch recoloring method, consider its effects on the LPRE distance. Having the source image I_1, the reference image I_2, and the destination image I_1', the LPRE distance of c_1 to I_1 is computed as:

$$\tau_{I_1}(\vec{\mathbf{c}}_1) = \|\vec{\mathbf{v}}_1^{\mathrm{T}}(\vec{\mathbf{c}}_1 - \vec{\eta}_1)\vec{\mathbf{v}}_1 - (\vec{\mathbf{c}}_1 - \vec{\eta}_1)\|. \tag{46}$$

Note that all images are considered to be homogeneous in this stage. Performing the same operation on the destination image we have

$$\tau_{I_1'}(\vec{\mathbf{c}}_1') = \|\vec{\mathbf{v}}_1'^{T}(\vec{\mathbf{c}}_1' - \vec{\eta}_1')\vec{\mathbf{v}}_1' - (\vec{\mathbf{c}}_1' - \vec{\eta}_1')\|. \tag{47}$$

Using (35) we have

$$\vec{\mathbf{c}}_1' - \vec{\eta}_2 = \mathbf{V_2}\mathbf{V_1}^{-1}(\vec{\mathbf{c}}_1 - \vec{\eta}_1). \tag{48}$$

Substituting (48) in (47) gives

$$\tau_{I_1'}(\vec{\mathbf{c}}_1') = \|\vec{\mathbf{v}}_2^{\mathrm{T}}\mathbf{V_2}\mathbf{V_1}^{-1}(\vec{\mathbf{c}}_1 - \vec{\eta}_1)\vec{\mathbf{v}}_2 - \mathbf{V_2}\mathbf{V_1}^{-1}(\vec{\mathbf{c}}_1 - \vec{\eta}_1)\|. \tag{49}$$

As $\vec{\mathbf{v}}_2$ is the first column of $\mathbf{V_2}$, and due to the equality in (42), we have

$$\vec{\mathbf{v}}_2 = \mathbf{V_2}\mathbf{V_1}^{-1}\vec{\mathbf{v}}_1. \tag{50}$$

Hence

$$\begin{aligned}\tau_{I_1'}(\vec{\mathbf{c}}_1') &= \|(\mathbf{V_2V_1}^{-1}\vec{\mathbf{v}}_1)^{\mathrm{T}}\mathbf{V_2V_1}^{-1}(\vec{\mathbf{c}}_1-\vec{\eta}_1)(\mathbf{V_2V_1}^{-1}\vec{\mathbf{v}}_1)\\ &\quad-\mathbf{V_2V_1}^{-1}(\vec{\mathbf{c}}_1-\vec{\eta}_1)\|\\ &= \|\vec{\mathbf{v}}_1^{\mathrm{T}}(\vec{\mathbf{c}}_1-\vec{\eta}_1)(\mathbf{V_2V_1}^{-1}\vec{\mathbf{v}}_1)-\mathbf{V_2V_1}^{-1}(\vec{\mathbf{c}}_1-\vec{\eta}_1)\|\\ &= \|\mathbf{V_2V_1}^{-1}[\vec{\mathbf{v}}_1^{\mathrm{T}}(\vec{\mathbf{c}}_1-\vec{\eta}_1)\vec{\mathbf{v}}_1-(\vec{\mathbf{c}}_1-\vec{\eta}_1)]\|. \end{aligned} \tag{51}$$

As both $\mathbf{V_1}$ and $\mathbf{V_2}$ are orthonormal matrices, the $\mathbf{V_2V_1}^{-1}$ matrix will be an orthonormal matrix as well. Thus, $\mathbf{V_2V_1}^{-1}$ reserves the length. Hence, (51) results in

$$\tau_{I_1'}(\vec{\mathbf{c}}_1') = \tau_{I_1}(\vec{\mathbf{c}}_1). \tag{52}$$

It directly results that the LPRE homogeneity criterion, the normalized LPRE (2), and the proposed fuzzification scheme (6), are all reserved under the proposed single-swatch recoloring.

As a result of above mentioned derivations, we proposed a single-swatch recoloring method that

- recolors a homogeneous swatch according to another homogeneous swatch.
- depends on no parameters.
- after the recoloring process, using the destination image as the reference image in another recoloring task results the same as using the original reference image. It means that the reference and the destination image are identical in color content.
- is completely invertible.
- is transitive.
- reserves LPRE distance, LPRE homogeneity criterion, LPRE normalized distance, and the LPRE-based fuzzification.
- is fast.

3.3.2. Recoloring color images

Consider the source image I_1 and the reference image I_2. Also, assume that we are given the set of homogeneous swatches $r_{11},\ldots,r_{1n}$ in the source image and the set of homogeneous swatches $r_{21},\ldots,r_{2n}$ in the reference image. The problem is to compute the destination image in the way that the transformed version of r_{1i} looks the same as r_{2i}, for $i=1,\ldots,n$.

Note that when using r_{1i} and r_{2i} as the source and the reference images to recolor the color vector $\vec{\mathbf{c}}_1$, the equation in (35) gives $\vec{\mathbf{c}}_{1\mathbf{i}}'$ (see Fig. 6). In fact, $\vec{\mathbf{c}}_{1\mathbf{i}}'$ is the recolorized vector given that $\vec{\mathbf{c}}_1$ is entirely belonging to r_{1i}. In this stage, we incorporate the fuzzyfication scheme proposed in Section 2 to blend the results

$$\begin{aligned}\vec{\mathbf{c}}_1' &= \frac{\sum_{i=1}^{n} h_{r_{1i},\beta}(\vec{\mathbf{c}}_1)\vec{\mathbf{c}}_{1\mathbf{i}}'}{\sum_{i=1}^{n} h_{r_{1i},\beta}(\vec{\mathbf{c}}_1)}\\ &= \frac{1}{\sum_{i=1}^{n} h_{r_{1i},\beta}(\vec{\mathbf{c}}_1)}\sum_{i=1}^{n} h_{r_{1i},\beta}(\vec{\mathbf{c}}_1)[\mathbf{V_{2i}V_{1i}}^{-1}(\vec{\mathbf{c}}_1-\vec{\eta}_{1\mathbf{i}})+\vec{\eta}_{2\mathbf{i}}]. \end{aligned} \tag{53}$$

Here, $\mathbf{V_{1i}}$, $\vec{\eta}_{1\mathbf{i}}$, $\mathbf{V_{2i}}$, and $\vec{\eta}_{2\mathbf{i}}$ denote the PCA matrix and the expectation vector of r_{1i} and r_{2i}, respectively. Deriving (53) we have

$$\vec{\mathbf{c}}_1' = \mathbf{V}\vec{\mathbf{c}}_1+\vec{\eta}, \tag{54}$$

where,

$$\mathbf{V} = \frac{\sum_{i=1}^{n} h_{r_{1i},\beta}(\vec{\mathbf{c}}_1)\mathbf{V_{2i}V_{1i}}^{-1}}{\sum_{i=1}^{n} h_{r_{1i},\beta}(\vec{\mathbf{c}}_1)}, \tag{55}$$

$$\vec{\eta} = \frac{\sum_{i=1}^{n} h_{r_{1i},\beta}(\vec{\mathbf{c}}_1)[\vec{\eta}_{2\mathbf{i}}-\mathbf{V_{2i}V_{1i}}^{-1}\vec{\eta}_{1\mathbf{i}}]}{\sum_{i=1}^{n} h_{r_{1i},\beta}(\vec{\mathbf{c}}_1)}. \tag{56}$$

This new notation shows that the proposed recoloring process is linear. For each pixel the destination vector is computed using the weighted sum of single swatch recoloring matrices and bias vectors. The experimental results are shown in Section 4.4.

4. Experimental results

All algorithms are developed in MATLAB 6.5, on an 1100 MHz Pentium III personal computer with 256 MB of RAM. the database contains 100 color images of size 512×512.

4.1. Color space dimension reduction for color images

To evaluate the energy compaction of the pc_i channels, a large set of homogeneous swatches were extracted from the test images. Fig. 7 shows eight samples adopted from parts of the four standard images of *Lena*, *Girl*, *Peppers*, and *Mandrill*. The test swatches are converted to the proposed 1-D representation and a few typical results are shown in Fig. 8. Numerical results are listed in Table 4. As clearly shown in Table 4, in contrast with the original color components with κ values around $\frac{1}{3}$, in the PCA channels, the information mostly gathers in the first channel (0.88 compared with 0.11 and 0.01). Comparison of κ_1 in the 1st and the 4th samples (the extreme values of κ_1) are noticeable too. While shades in the *nostrils* of the *Mandrill*, distributes the information in the three channels of PCA, the information densely focuses in pc_1 channel in the *hair* sample. This means that there is no relation between the spatial scattering pattern of the swatches and their energy compactions in the color domain.

The average PSNR value of 32 dB in Table 4 shows that the proposed dimension reduction process is a reasonable solution for homogeneous color vectors. Also, the low standard deviation of the PSNR values (4 dB) shows that the method responds uniformly. The highest PSNR value has been gained in the 5th sample, the *skin*. The worst result is obtained in the 1st sample because of the dark shades of the *nostrils*. Applying the proposed dimension reduction costs eight additions and four multiplications for each pixel.

Investigating the results of the proposed dimension reduction process shown in Fig. 8 demonstrates its

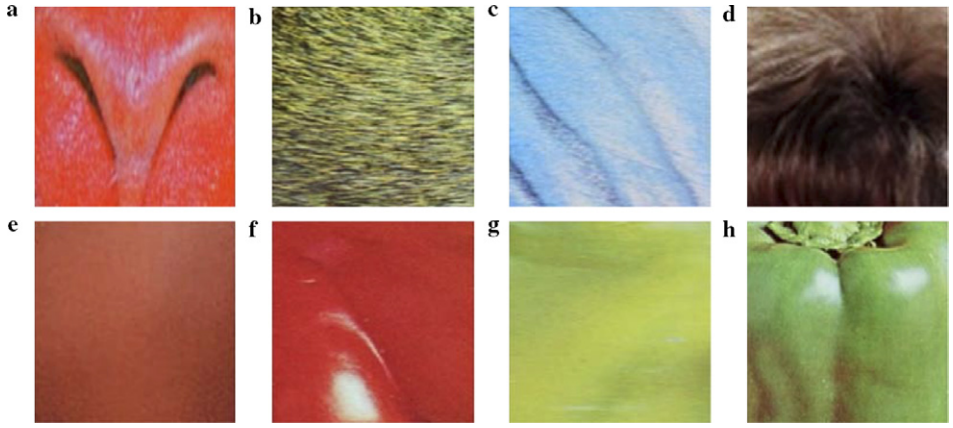

Fig. 7. Eight homogeneous regions in some standard images used for evaluating the proposed dimension reduction method. (a) Nose of *Mandrill*. (b) Wool of *Mandrill*. (c) Lateral part in nose of *Mandrill*. (d) Hair of *Girl*. (e) Skin of *Lena*. (f) Red pepper of *Peppers*. (g) Yellowish-Green pepper of *Peppers*. (h) Green pepper of *Peppers* (images are not proportionally resized). (For interpretation of the references to color in this figure legend, the reader is referred to the web version of this paper.)

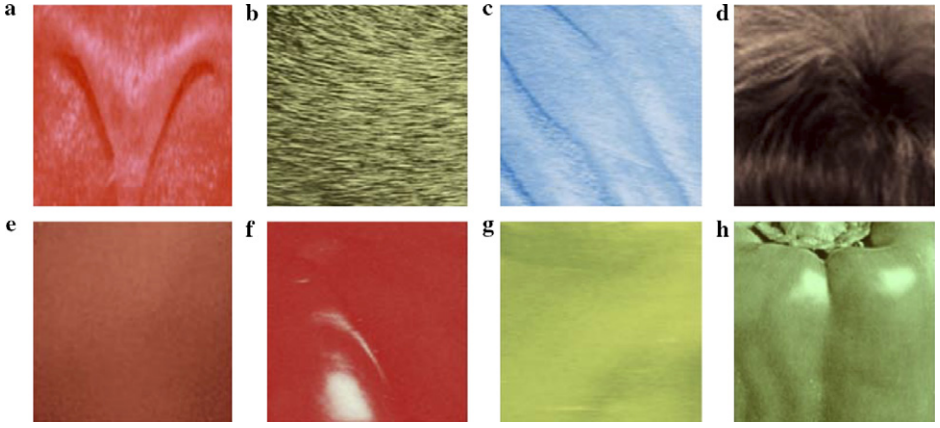

Fig. 8. Results of the proposed dimension reduction process applied on the samples shown in Fig. 7 (images are not proportionally resized). (For interpretation of the references to color in this figure legend, the reader is referred to the web version of this paper.)

Table 4
Numerical results of the proposed dimension reduction method

Swatch	PSNR (dB)	κ_{c_1}	κ_{c_2}	κ_{c_3}	κ_{pc_1}	κ_{pc_2}	κ_{pc_3}
(a)	25	0.28	0.20	0.52	0.72	0.26	0.02
(b)	30	0.34	0.38	0.28	0.96	0.04	0.00
(c)	30	0.63	0.22	0.15	0.80	0.20	0.00
(d)	35	0.42	0.32	0.23	0.99	0.01	0.00
(e)	38	0.41	0.31	0.28	0.95	0.05	0.00
(f)	34	0.04	0.51	0.45	0.97	0.03	0.00
(g)	33	0.46	0.29	0.25	0.78	0.20	0.02
(h)	28	0.18	0.42	0.40	0.89	0.08	0.03
η	32	0.35	0.33	0.32	0.88	0.11	0.01
σ	4	0.18	0.10	0.12	0.10	0.10	0.01

subjective performance. Thus, according to the typical results stated here and the numerous results of other sample images (not shown here due to length constrain), it is concluded that the proposed dimension reduction method performs reasonable for homogeneous swatches of the color images of the nature.

4.2. Color image fuzzification

Fig. 9 shows the results of the proposed fuzzification method on the sample image *Peppers*. The corresponding β values are denoted in the caption of Fig. 9. Here, the query region is a rectangular part of the red pepper (see Fig. 9a). This sample is only shown here as a typical example. For full discussion see [20].

4.3. Grayscale image colorizing

Fig. 10 shows the segmented version of the three standard images of *Lena*, *Girl*, and *Barbara* along with some samples adopted from Welsh et al. [1] and Levin et al. [5]. The segmentation is performed manually with repeatedly using the *magic select* tool in *Adobe Photoshop* into six distinct segments like the *skin*, *hair*, *lip*, *cloth*, and the forth.

Fig. 11 shows the results of applying the two proposed colorizing methods of (23) and (24) on the two samples of Welsh et al. [1] along with the results of their method.

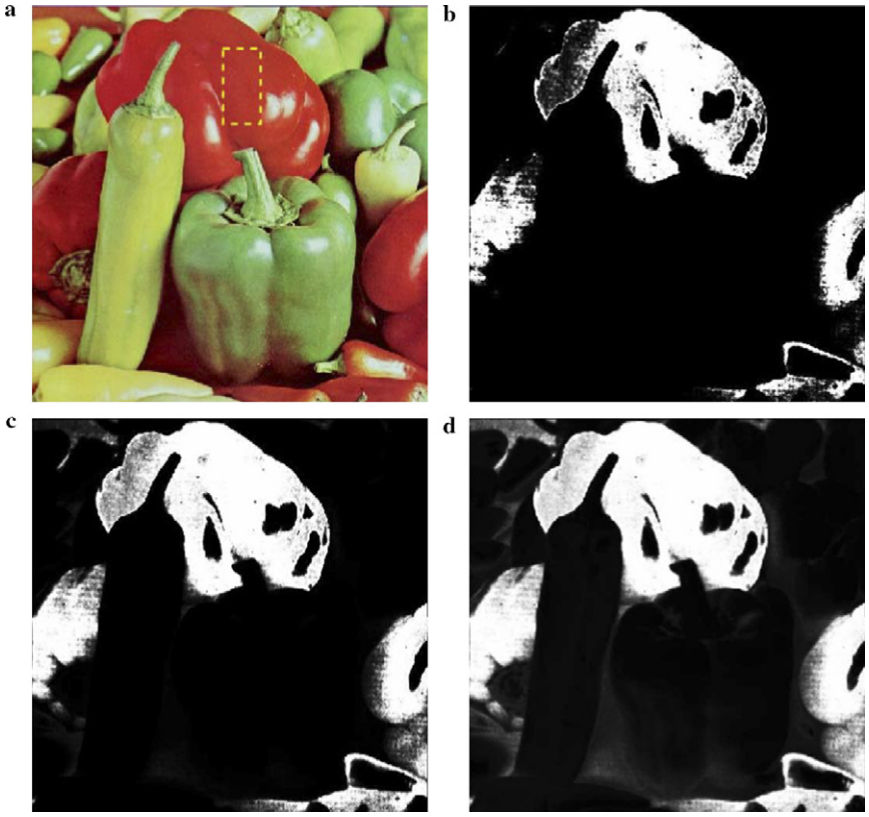

Fig. 9. Fuzzification of *Peppers* according to the shown query region with different values of β. (a) Original image overlayed the query region. (b) $\beta = 0.1$. (c) $\beta = 0.6$.(d) $\beta = 0.9$. (For interpretation of the references to color in this figure legend, the reader is referred to the web version of this paper.)

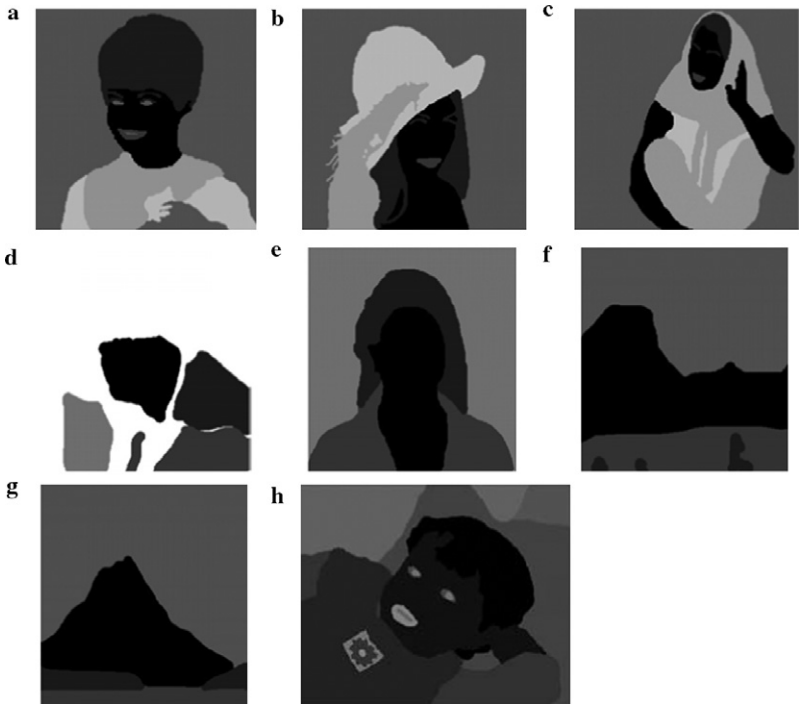

Fig. 10. Segmented version of test images. (a) *Girl*. (b) *Lena*. (c) *Barbara*. (d–g) Adopted from Welsh et al. [1]. (h) Adopted from Levin et al. [5].

The subjective test of goodness on Welsh et al. [1] samples gave the following results. When the average score for Welsh et al.'s algorithm [1] is 1.833, the method in (23) is scored 2.119 and (24) is given 2.429 making the average score for the proposed methods about 2.27 (all out of 3). Thus, the proposed methods are recognized subjectively,

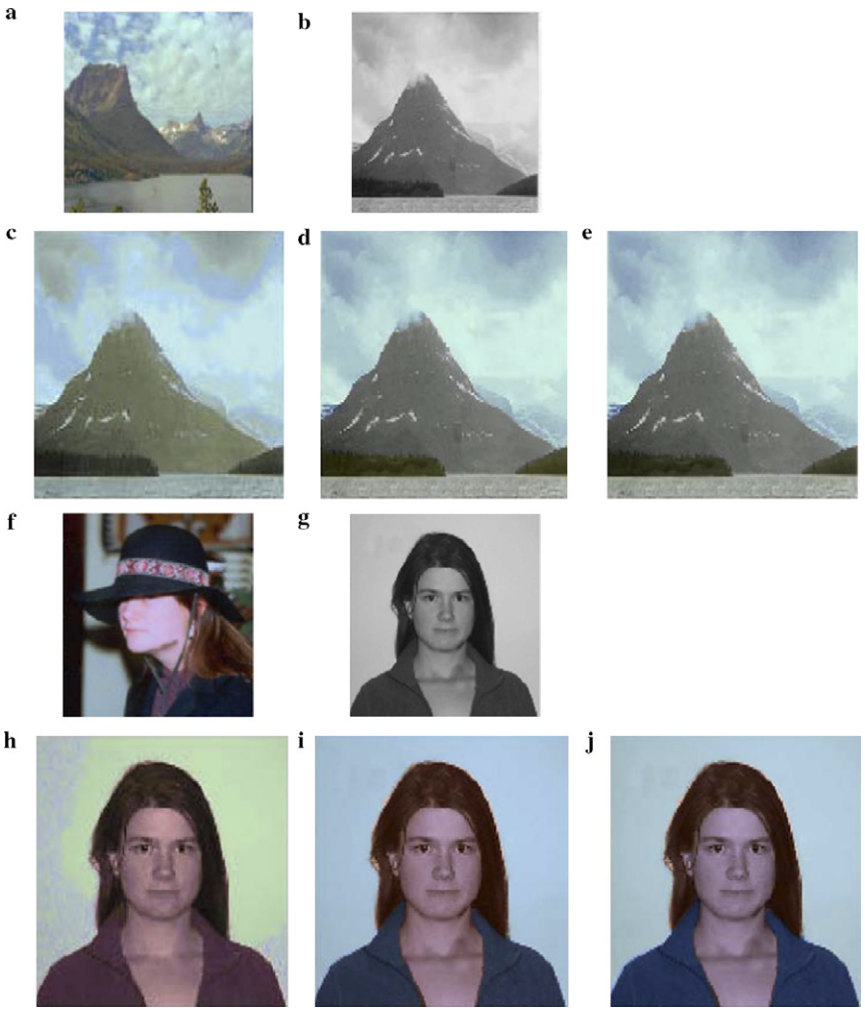

Fig. 11. Two samples of Welsh et al. [1] along with the results of the proposed methods. (a) and (f) reference images. (b) and (g) source images. (c and h) Results of Welsh et al. [1]. (d and i) Results of the proposed method in (23). (d and j) Results of the proposed method in (24). (a–c, f–h) Adopted from Welsh et al. [1]. (For interpretation of the references to color in this figure legend, the reader is referred to the web version of this paper.)

16 and 32% better than Welsh et al.'s results [1], respectively. This results in 24% better scores in average. Also, the second proposed method is about 15% better than the first method.

Welsh et al. [1] use the luminance as the segmentation criterion. Hence, their method is completely dependence on the similarity of the source and the reference images in the grayscale domain. Using the intensity as the matching feature makes an odd perceptual artifact in Welsh et al.'s [1] synthesized images as a discontinuity in color appearance. Such effect can be easily recognized in the background of the samples shown in Figs. 11c and h and other samples shown in [1]. Also, the proposed methods perform the PCA for each sample; in contrast with Welsh et al.'s [1] work that uses the $\ell\alpha\beta$ color space that is based on performing the PCA on a set of sample images to derive the color space formulation. Therefore, (theoretically) we are working on a better base of uncorrelatedness.

The three conditions defined in Section 3.2 are a ground-truth for new colorizing algorithms. The first proposed method, justifies only two of the conditions, where the second proposed method justifies all. Welsh et al.'s [1] method holds the first condition, as he just transfers α and β components, leaving the ℓ value unchanged but they have given no attention to the two other conditions. It must be emphasized that the ℓ component of $\ell\alpha\beta$ is not a linear norm function.

The proposed method works about 60 times faster than Welsh et al.'s method [1]. The proposed methods averagely elapses less than 2 s whilst Welsh [1] has reported a 15 s to 4 min record in similar platforms, though they offer to use larger neighborhood windows to enhance the results. Table 5 lists the comparison result between Welsh et al.'s work [1] and the proposed algorithms. The grayscale version of the three face images, *Lena*, *Girl*, and *Barbara* (see Fig. 12), are colorized 12 times, once using *Lena* as the reference image and then using *Girl* for this purpose, each colorization performed twice, once by (23) and then by (24). A subjective test was performed on the results, containing two questions of impairment (see Table 2) and goodness (see Table 3). As the background is retained grayscale in all synthetic images, the background of the original images were made

grayscale before exposure to the test subjects. To find out the method's performance when dealing with the special problem of face colorizing, both questions are asked twice, once for the entire image and then only for the face area. As the color version of *Barbara* is not available, only the goodness question is asked regarding this image. To measure the quality of the proposed colorizing schemes, sample color images are converted to grayscale and then colorized by their own color information or that of others. doing as such, the PSNR values of colorizing *Lena* and *Girl* (with each other) in both proposed methods are listed in Table 6. For a 256×256 image containing eight regions, the color

Table 5
Performance comparison of Welsh et al.'s colorizing method [1] with the two proposed methods

Method	Goodness $(1, \ldots, 3)$	Criterion			Elapsed time
		I	II	III	
Welsh et al. [1]	1.83	√	—	—	15 s to 4 min
Proposed (23)	2.12	√	—	√	2*s*
Proposed (24)	2.43	√	√	√	2*s*

Table 6
PSNR values for *Lena* and *Girl* colorizing tests, using different methods

Reference:	*Lena*		*Girl*	
Method:	(23)	(24)	(23)	(24)
Source (dB)				
Lena	26	26	18	21
Girl	14	13	28	28

Table 7
Subjective tests of colorizing process, all values are out of 100

Condition	Method	Image		Face	
		Impairment	Goodness	Impairment	Goodness
$M = S$[a]	(23)	67	75	82	90
	(24)	75	87	88	98
$M \neq S$[b]	(23)	35	72	45	80
	(24)	40	83	52	96
No S[c]	(23)	—	60	—	80
	(24)	—	78	—	95

[a] Reference image is the colored version of the source image.
[b] Another image is used as the reference image.
[c] Colored version of the source image is not available.

Fig. 12. Results of the proposed colorizing methods. (a, b, e, f, i, and j) Reference image is *Lena*. (c, d, g, h, k, and l) Reference image is *Girl*. (a, e, i, c, g, and k) Colorized by (23). (b, d, f, h, j, and l) Colorized by (24). (For interpretation of the references to color in this figure legend, the reader is referred to the web version of this paper.)

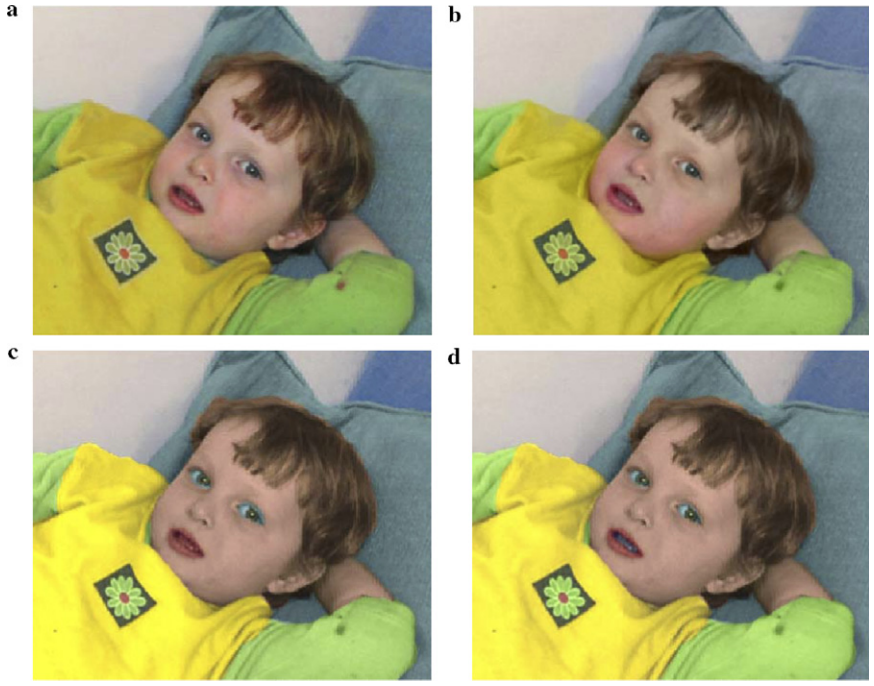

Fig. 13. Comparison of the proposed colorizing methods with the method by Levin et al. [5]. (a) Original image adopted from Levin et al. [5]. (b) Result of [5]. (c) Result (23). (d) Result of (24). (For interpretation of the references to color in this figure legend, the reader is referred to the web version of this paper.)

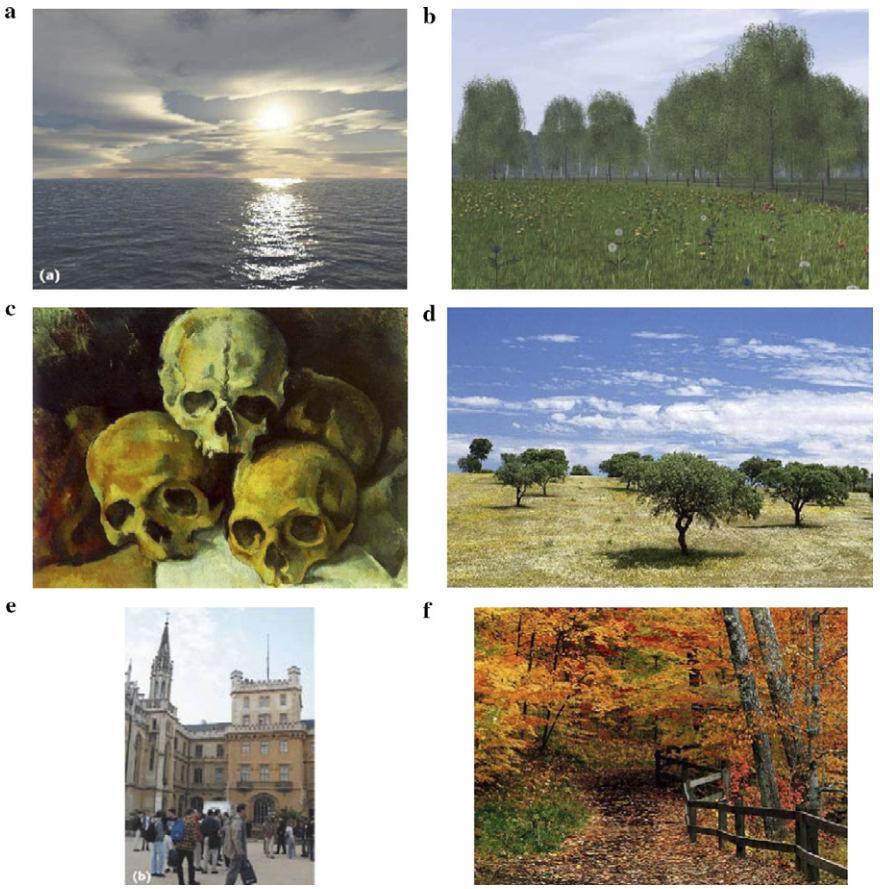

Fig. 14. Source images. (a, b, and e) Adopted from Reinhard et. al. [8]. (c) Adopted from Greenfield et al. [11]. (d) Adopted from Chang et al. [10]. (f) Adopted from www.webshots.com with permission of the authors, ''Mc. Cormic Creck State Park, Indiana'' by Mike Briner, mbphoto@spraynet.com, www.mikebrinerphoto.com. (For interpretation of the references to color in this figure legend, the reader is referred to the web version of this paper.)

extraction phase is performed in 2 s averagely, when the color transfer phase got another 2 s. Results of subjective test on face colorizing scaled to the range of $[0, \ldots, 100]$ are listed in Table 7. Table 6 shows that the two proposed methods are similar in the PSNR sense. It is clear that colorizing each image by its color information gives better results, though the meaning of the PSNR test must be considered carefully. Many objectionable images with high values of PSNR can be produced. In face images, the proposed methods are approximately scored 83 out of 100, which means that the synthetic images are averagely perceived "good". In impairment scales, the colorized images are considered "not objectionable" (60.5 out of 100). Face region is averagely ranked 23% higher than the whole colorized area and the method proposed in (24) is ranked 18% better than (23). Also, it must be emphasized that colorizing an image with its own color content gives better results, but not much better though (less than 6%). In the PSNR sense, colorizing a color image using its own color information is massively outperforming the case of colorizing a color image using a different reference image.

Fig. 13 shows the comparison of the proposed colorizing method with the method by Levin et al. [5]. Their method elapses 15 s on each image compared to less than 2 s record of the proposed methods. Comparing the visual appearance of the results, their method is performing better in the edges because of the interpolation scheme that they are using. We propose to use their novel optimization framework combined with the proposed PCA-based color generation stage to reach better results. In terms of the defined criteria, the method by Levin et al. [5] fulfills the first condition (not altering the original grayvalue) but fails the two others.

4.4. Color transfer between images

Figs. 14 and 15 show some of the sample images used for evaluating the performance of the proposed colorizing method. The proposed color transform method is performed on some typical sample images shown in Fig. 14. The results of the proposed method along with the results of other available methods are shown in Fig. 16. The β values and the description of the selected regions in images are expressed in the caption of Fig. 16. It is worth to note that transferring color information of a 512×512 image into a 512×512 image according to four selected medium-sized base swatches elapses less than 2 s. Comparing the results shown in Figs. 16 and 17 shows the difference among various algorithms. Figs. 17a, b, and f show sample results of

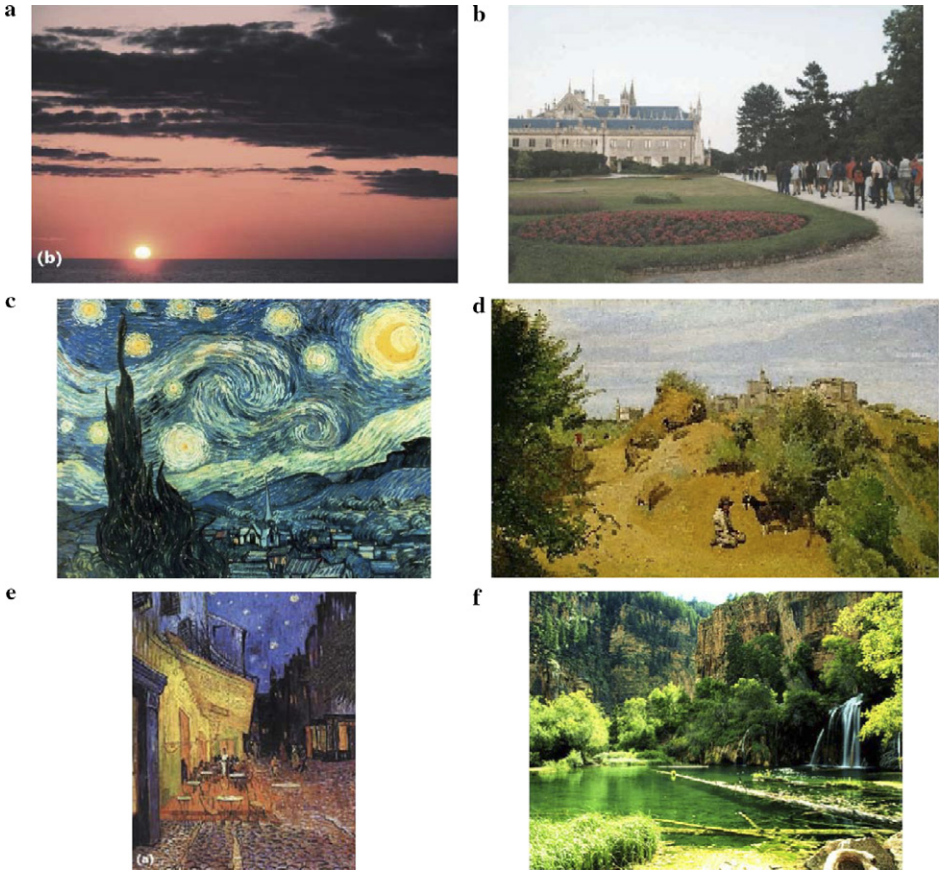

Fig. 15. Reference images. (a, b, and e) adopted from Reinhard et al. [8]. (c) Adopted from Greenfield et al. [11]. (d) Adopted from Chang et al. [10]. (f) Adopted from www.webshots.com with permission of the authors, "Hanging Lake" by Brent Reed, brent@reedservices.com. (For interpretation of the references to color in this figure legend, the reader is referred to the web version of this paper.)

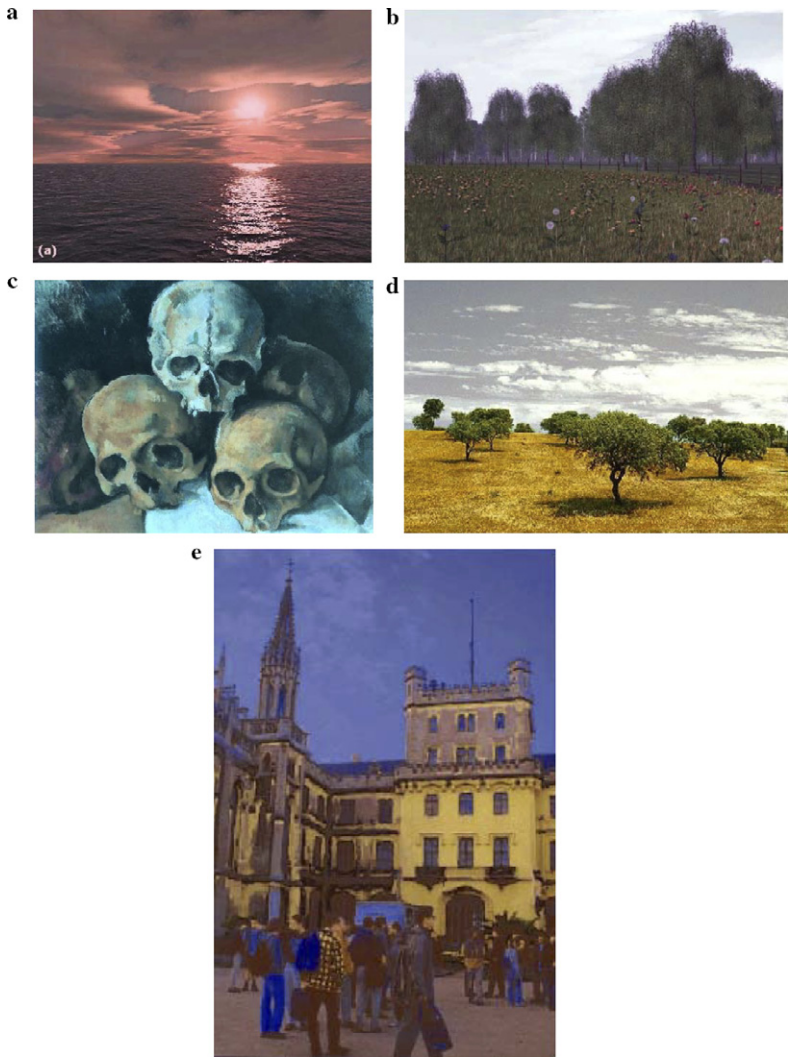

Fig. 16. Results of the proposed recoloring method applied on sample images shown in Figs. 14 and 15. Source images are shown in Figs. 14a–e, respectively. Reference images are shown in Figs. 15a–e, respectively. Used settings are (a) $\beta = 0.95$, $R = \{Sky, Water\}$, (c) $\beta = 0.1$, $R = \{Leaves, Sky\}$, (c) $\beta = 0.8$, $R = \{Skulls, Background\}$, (d) $\beta = 0.5$, $R = \{Leaves, Sky, Earth\}$, and (e) $\beta = 0.95$, $R = \{Sky, Building, Pavement\}$. (For interpretation of the references to color in this figure legend, the reader is referred to the web version of this paper.)

Reinhard et al. [8]. Comparing Fig. 17a with Fig. 16a shows that the results of the proposed method and that method are almost similar. In Fig. 17b, the differences are clear. Reinhard et al.'s [8] method have changed the color of the whole image to the same greenish mood, resulting in blurring the strong edges between the trees and the sky. Also, the blue sky in Fig. 17b has nothing to do with the entirely white sky of Fig. 15b. In addition, the method in [8] has eliminated the red flowers. In contrast, the result of the proposed method in Fig. 16b shows no blurring and proper color contrast. Also, the warm colors of the red flowers are completely reserved. Although, Greenfield's method [11] has tried to transfer the cold colors of Fig. 15c to Fig. 14c, but Fig. 17c still contains the warm violet-blue colors on the topmost skull. In the result of the proposed method shown in Fig. 16e, the colors are mostly cold. Fig. 17d shows the result of the method by Chang et al. [10] which is almost acceptable but lacks proper color contrast. Returning back to Reinhard et al.'s method [8], there is a discontinuity artifact in the sky in Fig. 17e. Note that, the sky in Fig. 16e simulates a real night sky having in mind that the photograph has taken at daytime. This fact is more desiring when one confirms that the recolorized image by the method in [8], shown in Fig. 17e, does not seem to be a night scene while Fig. 16e does seem so.

Although, transferring the color information of a real image to a painting and vice versa is possible, but one must consider the meaning of such transformation thoughtfully. While the color information in a real photograph is a continually changing vector, it is a regional almost constant information in a painting (due to the process that has made it; the brush with a unique color moves on the canvas). Furthermore, using a reference image of entirely different scene compared with the source image does not make the process to fail, but the results of such operation must be

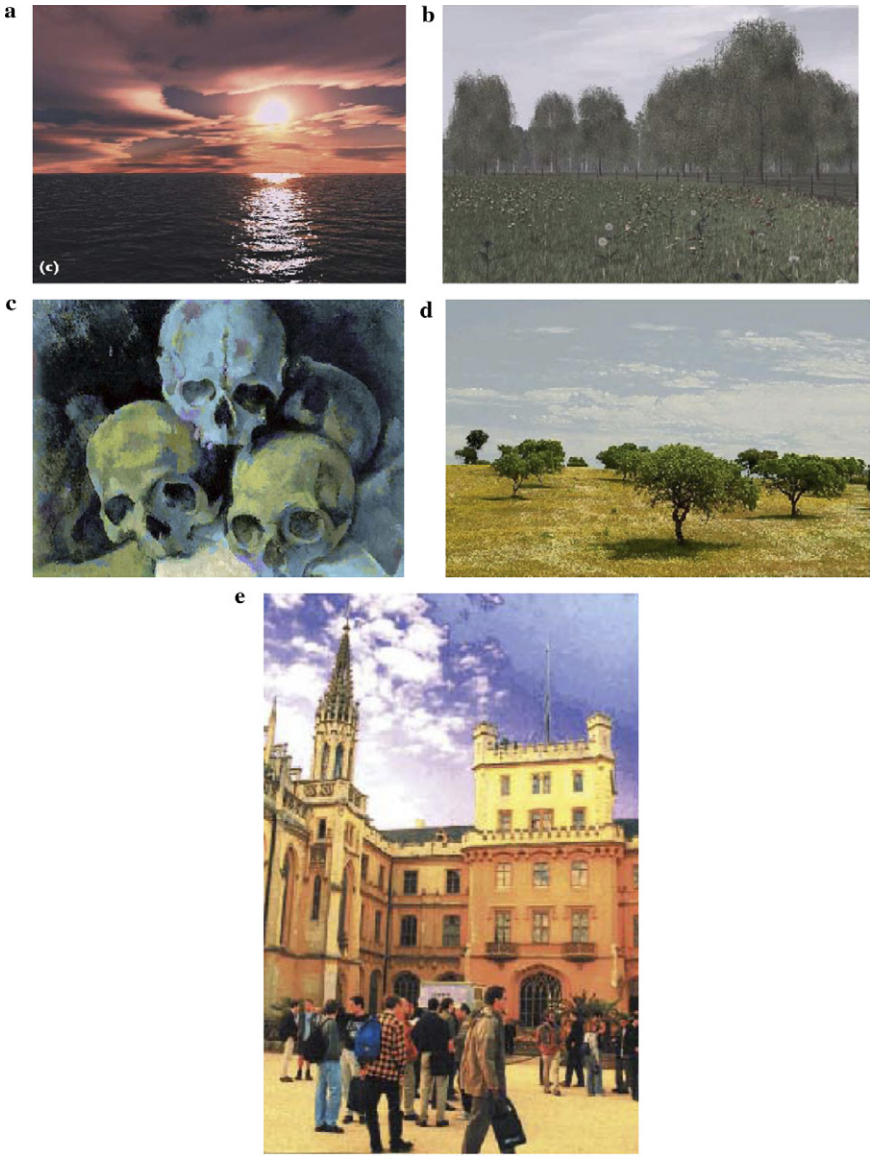

Fig. 17. Results of other available methods applied on sample images of Figs. 14 and 15. Source images are shown in Figs. 14a–e, respectively. Reference images are shown in Figs. 15a–e, respectively. (a), (b), and (e) method in [8]. (c) Method in [11]. (d) Method in [10]. (For interpretation of the references to color in this figure legend, the reader is referred to the web version of this paper.)

deliberated carefully. The same event occurs when giving regions of the source image and the reference image in a scattered fashion; for example trying to transfer color information of leaves to sand. The exact report of the time measurement is neglected in the references but considering the less than two seconds record of the proposed method while other methods use sophisticated methods of segmentation and convex hull computation, the outperforming results of the proposed method is clear. It must be emphasized that in the proposed methods, using an image as source image and reference image at the same time (recoloring an image with itself as the reference image), when working on almost the same regions in the reference image and the source image, results in an image that cannot be recognized from the original image. In addition, when using single-swatch version of the method, the process is completely revertible. Although in all samples discussed above the reference image is unique, there is no limitation that prevents the user from using two or more images as the reference image. That is because the proposed method is not actually using the reference image, but it needs a set of homogeneous swatches. This option may be useful when trying to recolor a source image due to the sky in the first reference image and the leaves in the second reference image two. Such an option is available in the method in [8] but not in the methods in [11,10].

The proposed method needs a set of homogeneous swatches in the two images as the reference for the transform and a single β parameter that controls the averaging of the color vectors. We wish to emphasize that this is the minimal set given for this problem. The methods in [10,11] transfer the color information based on a set

Fig. 18. Results of the proposed colorizing method. (a) Reference image. (b) Source image. (c) Result of the proposed recoloring method ($\beta = 0.2$, $R = \{Leaves, Bushes, Bark\}$). (For interpretation of the references to color in this figure legend, the reader is referred to the web version of this paper.)

of fixed color categories or some spatial cues, leaving no room for user intervention. What we really need from a proper color transfer methods is to let the user intentionally select a set of relations in the color domain and ask the method to perform the suitable transformation. Such an input to the algorithm can be eliminated if we reach upon intelligent algorithms that automatically understand the image contents to find the relation among the scene materials. We are insisting that it is not the shortage of an algorithm but it is its user friendliness to make him able to give his intention. The β parameter is the one neglected in available recoloring methods. It professionally controls the blurring attitude of the method. Due to different imaging conditions, it is probable that the reference and the source images be in different conditions of edges. Then, by using the β value, one can compensate these differences.

To make the power of the proposed color transform process more clear, the source image of Fig. 14f and the reference image of Fig. 15f are shown in Fig. 18 again, along with the recolorized version.

5. Conclusion

In this paper, a new and efficient PCA-based dimension reduction method for homogeneous color swatches is proposed and its performance is analyzed. The results along with other works discussed here, show that the PCA gives a proper model for color vectors of homogeneous swatches. A new colorizing method is proposed that uses the proposed dimension reduction method. Then, using the same ideas, a recoloring method is proposed and the performance of both proposed methods are carefully compared with that of other available algorithms. The proposed methods are shown to be dominantly faster than the available approaches while resulting in more acceptable results. One of the main contributions of this paper is giving a unifying approach for the two aspects of color transfer (colorizing and recoloring).

Acknowledgments

We appreciate the anonymous referees for their constructive suggestions and the participants of the subjective tests for their patience. The first author also thanks Ms. Azadeh Yadollahi for her encouragement and invaluable ideas.

References

[1] T. Welsh, M. Ashikhmin, K. Mueller, Transferring color to grayscale images, in: Proceedings of ACM SIGGRAPH 2002, San Antonio, 2002, pp. 277–280.
[2] W.-Q. Yan, M.S. Kankanhalli, Colorizing infrared home videos, in: Proceedings of IEEE International Conference on Multimedia and Expo (ICME 2003), Baltimore, 2003.
[3] L.F.M. Vieira, R.D. Vilela, E.R. do Nascimento, F.A.F. Jr., R.L. Carceroni, A. de A. Araujo, Automatically choosing source color images for coloring grayscale images, in: Proceedings of the XVI Brazilian Symposium on Computer Graphics and Image Processing (SIBGRAPI'03), Sao Carlos, Brazil, 2003, pp. 151.
[4] T. Horiuchi, S. Hirano, Colorization algorithm for grayscale image by propagating seed pixels, in: IEEE International Conference on Image Processing (ICIP'03), 2003, pp. 457–460.
[5] A. Levin, D. Lischinski, Y. Weiss, Colorization using optimization, ACM Transactions on Graphics, 2004.
[6] T. Chen, Y. Wang, V. Schilings, C. Meinel, Grayscale image matting and colorization, in: Proceedings of ACCV2004, Jeju Island, Korea, 2004, pp. 1164–1169.
[7] R. Gonzalez, P. Wintz, Digital Image Processing, Addison-Wesley, Reading, MA., 1987.

[8] E. Reinhard, M. Ashikhmin, B. Gooch, P. Shirley, Color transfer between images, IEEE Computer Graphics and Applications (2001) 34–41.
[9] L. Yin, J. Jia, J. Morrissey, Towards race-related face identification: research on skin color transfer, in: Proceedings of the Sixth IEEE International Conference on Automatic Face and Gesture Recognition (FGR'03), 2003.
[10] Y. Chang, S. Saito, M. Nakajima, A framework for transfer colors based on the basic color categories, in Proceedings of the Computer Graphics International (CGI'03), IEEE, 2003.
[11] G.R. Greenfield, D.H. House, Image recoloring induced by palette color associations, Journal of WSCG'03 11 (1) (2003) 3–7.
[12] D. Ruderman, T. Cronin, C. Chiao, Statistics of cone response to natural images: implementation for visual coding, Optical Doc. of America 15 (8) (1998) 2036–2045.
[13] T. Horiuchi, Colorization algorithms using probabilistic relaxation, Image and Vision Computing 22 (2004) 197–202.
[14] D. Sykora, Inking old black and white cartoons, Master's thesis, Department of Computer Science and Engineering, FEE, CTU, Prague, Czech Republic, 2003.
[15] D. Sykora, J.B.J. Zara, Unsupervised colorization of black-and-white cartoons, in: NPAR'04, 2004.
[16] B. Berlin, P. Kay, Basic Color Terms, Their Universality and Evolution, University of California Press, Berkeley, 1969.
[17] M.-H. Yang, D.J. Kriegman, M. Ahuja, Detecting faces in images: a survey, IEEE Transactions on Pattern Analysis ad Machine Intelligence 24 (1) (2002) 34–58.
[18] M.C. Shin, K.I. Chang, L.V. Tsap, Does color space transformation make any difference on skin detection?, in: IEEE Workshop on Applications of Computer Vision, Orlando, FL, 2002, pp. 275–279.
[19] S. Jayaram, S. Schmugge, M.C. Shin, L.V. Tsap, Effect of color space transformation, the illuminance component, and color modelling on skin detection, in: 2004 IEEE Computer Society Conference on Computer Vision and Pattern Recognition (CVPR'04), 2004.
[20] A. Abadpour, S. Kasaei, Performance analysis of three likelihood measures for color image processing, in: IPM Workshop on Computer Vision, Tehran, Iran, 2004.
[21] G.J. Klinker, S.A. Shafer, T. Kanade, The measurement of highlights in color images, International Journal of Computer Vision 2 (1988) 7–32.
[22] G.J. Klinker, S.A. Shafer, T. Kanade, A physical approach to color image understanding, International Journal of Computer Vision 4 (1990) 7–38.
[23] S.-C. Cheng, S.-C. Hsia, Fast algorithm's for color image processing by principal component analysis, Journal of Visual Communication and Image Representation 14 (2003) 184–203.
[24] D.O. Nikolaev, P.O. Nikolayev, Linear color segmentation and its implementation, Computer Vision and Image Understanding 94 (2004) 115–139.
[25] M. Turk, A. Pentland, Eigenfaces for recognition, Journal of Cognitive Neuroscience 3 (1) (1991) 71–86.
[26] N. Papamarkos, C. Strouthopoulos, I. Andreadis, Multithresholding of color and gray-level images through a neural network technique, Image and Vision Computing 18 (2000) 213–222.
[27] D. Tschumperle, Pde's based regularization of multivalued images and applications, Ph.D thesis, University of Nice, Sophia Antipolis, 2002.
[28] H. Cheng, J. Li, Fuzzy homogeneity and scale-space approach to color image segmentation, Pattern Recognition 36 (2003) 1545–1562.
[29] J. Bruce, T. Balch, M. Veloso, Fast and cheap color image segmentation for interactive robots, in: Proceedings of IROS-2000, Japan, 2000.
[30] T. Chaira, A. Ray, Fuzzy approach for color region extraction, Pattern Recognition 24 (2003) 1943–1950.
[31] L. Lucchese, S. Mitra, Colour segmentation based on separate anisotropic diffusion of chromatic and achromatic channels, Vision, Image, and Signal Processing 148 (3) (2001) 141–150.
[32] A. Abadpour, S. Kasaei, A new parametric linear adaptive color space and its pca-based implementation, in: The 9th Annual CSI Computer Conference, CSICC, Tehran, Iran, 2004, pp. 125–132.
[33] A. Abadpour, S. Kasaei, A new pca-based robust color image watermarking method, in: The 2nd IEEE Conference on Advancing Technology in the GCC: Challenges, and Solutions, Manama, Bahrain, 2004.
[34] A. Abadpour, S. Kasaei, A new fpca-based fast segmentation method for color images, in: The 4th IEEE International Symposium on Signal Processing and Information Technology (ISSPIT 2004), Rome, Italy, 2004.
[35] Y.I. Ohta, Y. Kanade, T. Saki, Color information for region segmentation, Computer Graphics and Image Processing 13 (No.3) (1980) 222–241.
[36] J. Tenenbaum, T. Garvey, S. Weyl, H. Welf, An interactive facility for scene analysis research, Tech. Rep. 87, Stanford Research Institute, AI Center, 1974.
[37] J. Foley, A. Van Dam, Fundamentals of Interactive Computer Graphics, The System Programming Series, Addison-Wesley, Reading, MA, 1982, Reprinted 1984 with corrections.
[38] J. Slater, Modern Television System to HDTV and Beyond, Pitman, London, 1991.
[39] K. Benson, Television Engineering Handbook, Mc Graw-Hill, New York, London, 1992.
[40] ITU-R Recommendation BT-601-5: Studio Encoding Parameters of Digital Television for Standard 4:3 and Widescreen 16:9 Aspect Ratios, www.itu.ch/, Geneva, 1994.
[41] A.K. Jain, Fundamentals of Digital Image Processing, Prentice-Hall International, Republic of Sigapore, 1989.
[42] A. Abadpour, S. Kasaei, A new principle component analysis based colorizing method, in: Proceedings of the 12th Iranian Conference on Electrical Engineering (ICEE2004), Mashhad, Iran, 2004.
[43] A. Abadpour, S. Kasaei, A new fast fuzzy color transfer method, in: The 4th IEEE International Symposium on Signal Processing and Information Technology (ISSPIT 2004), Rome, Italy, 2004.